ELSEVIER

Journal of Structural Geology 26 (2004) 1043–1065

JOURNAL OF STRUCTURAL GEOLOGY

www.elsevier.com/locate/jsg

How to resolve the controls on mesothermal vein systems in a goldfield characterized by sparse kinematic information and fault reactivation—a structural and graphical approach

Oliver P. Kreuzer*

Economic Geology Research Unit (EGRU), School of Earth Sciences, James Cook University, Queensland 4811, Australia

Received 1 November 2002; received in revised form 26 June 2003; accepted 13 July 2003

Abstract

Current mine exposures of auriferous veins in the Charters Towers Goldfield (CTGF) are characterized by a scarcity of kinematic indicators. Furthermore, the dip direction of exposed and historically mined orebodies largely coincides with the orientation of pre-existing discontinuities. Consequently, the reactivation of earlier structures during gold deposition is strongly indicated. Both factors complicate the structural analysis of the auriferous vein systems, as slip on earlier faults likely occurred before new rock failure and evolution of fault networks reflecting the stress field present at the time of gold deposition. Despite access to drillcore, open pits and underground workings, extracted data were limited to ten occurrences of wear groove striations and three reverse separations of dykes and a pegmatite cut by sulphide-bearing quartz veins. Because of the scarcity of kinematic information, the structural analysis focused on the geometry of veins and ore-shoots, also applying basic graphical and kinematic methods.

Keywords: Mesothermal gold deposits; Structural and graphical analysis; Reactivation; Charters Towers

1. Introduction

Based on their geological setting, mineralogy, and geochemical signature, vein systems in the Charters Towers Goldfield (CTGF) have been referred to as mesothermal (Lindgren, 1933), synorogenic Pacific Rim-type (Goldfarb et al., 1998) or orogenic (Groves et al., 1998; Goldfarb et al., 2001) deposits of Palaeozoic age. Historic production (1872–1969) from auriferous veins in the CTGF exceeded 6.5 Moz Au (Levingston, 1972) making Charters Towers one of the largest Australian goldfields (Solomon and Groves, 2000) with >6 million tons of extracted ore yielding an average grade of 34 g/t Au (Blatchford, 1953; Levingston, 1972). At present Charters Towers Gold Mines Ltd are exploring for ore-shoot repetitions underneath several historic workings at Charters Towers. SMC Gold Ltd are mining and exploring for resources along the 'Rishton–Hadleigh Castle Corridor'.

The current study combined regional mapping, drillcore and deposit studies in the Charters Towers and Hadleigh Castle areas and aimed to evaluate the role of reactivation of pre-existing discontinuities during quartz vein formation and gold deposition. It also aimed to clarify the orientation of the regional strain field during Siluro-Devonian gold mineralization. An understanding of the mode of faulting and the strain field present at the time of ore deposition is of importance to mineral exploration, as it assists with the identification of dilational and restraining sites that may have been favorable for enhanced fluid flow and mineralization within the fold, foliation and fracture array (e.g. Sibson, 2001; Allibone et al., 2002) of the region, which is characterized by a multiphase deformation history.

The literature on lode gold deposits generally contains a reasonable amount of structural information (e.g. Hodgson, 1989; Cox et al., 1991; Cassidy and Bennet, 1993; Forde and Bell, 1994; McKeagney et al., 1997; Vearncombe, 1998; Robert and Poulsen, 2001; Miller and Wilson, 2002) whereas the vein systems currently accessible in the CTGF are characterized by a scarcity of kinematic indicators. The paucity of striations, vein intersections and cross-cutting relationships appears to be related to a number of factors: (a) many of the open cut exposures are affected by significant degrees of weathering and kinematic indicators, if originally present, were probably lost to that destructive process, (b) lower pit levels are often water-filled and thus inaccessible, (c) the granitic wallrocks are often devoid of structural information, and (d) significant exposures may have been

* Tel.: +61-7-4781-6153; fax: +61-7-4725-1501.
E-mail address: Oliver.Kreuzer@jcu.edu.au (O.P. Kreuzer).

0191-8141/$ - see front matter © 2004 Elsevier Ltd. All rights reserved.
doi:10.1016/j.jsg.2003.11.007

removed by mining. Reid's (1917) observations of abundant slickensided wallrocks and cross-cutting relationships in the historic mines support the significance of the latter factor. However, the current study benefited greatly from the mine exposures that were not available to recent workers (Peters, 1987a,b; Peters and Golding, 1989), whose investigations were restricted to scattered surface outcrop and widely spaced drillcore. As a result, their structural analyses were largely based on information gathered from historic maps, records and mining plans compiled by Jack et al. (1898), Reid (1917) and Levingston (1972). The structural analysis of the vein systems was also complicated by the pre-existing structure of the host rocks and potential reactivation of earlier discontinuities during gold mineralization.

2. Regional geology

2.1. Geological background and tectonic setting

The study areas at Charters Towers and Hadleigh Castle (Fig. 1) are situated in the Palaeozoic Ravenswood Batholith (RAB), a composite igneous body consisting mainly of oxidized (magnetite-series) and hornblende-bearing I-type granitoids (e.g. Richards, 1980). The RAB crops out over $>6000\ km^2$ of a largely concealed Neoproterozoic to Palaeozoic region, variously named as the Lolworth–Ravenswood Block (Murray and Kirkegaard, 1978), Province (Henderson, 1980; Hutton et al., 1997) or Terrane (Scheibner and Veevers, 2000), which forms an E–W-trending element within the N–S to NNW–SSE striking Tasman Fold Belt System.

The RAB intrusions were emplaced into a composite basement. To the north, it consists of greenschist to amphibolite-grade metasedimentary and meta-igneous rocks of Proterozoic to Cambrian age. In contrast, greenschist or lower-grade volcanics and sediments of Cambrian to Ordovician age dominate the southern basement. The intrusive history of the RAB commenced at the Cambro-Ordovician boundary and has been divided into Early to mid-Ordovician, mid-Silurian to mid-Devonian and Late Carboniferous to Early Permian phases of magmatic activity. Early to mid-Ordovician felsic to intermediate intrusions (490 ± 6 to 463 ± 3 Ma) are spatially associated with poorly known gabbroic to dioritic bodies that are thought to represent remnants of a mafic underplate. Following a mid-Ordovician to mid-Silurian time of deformation and limited igneous activity, mid-Silurian to mid-Devonian magmatism (426 ± 4 to 382 ± 5 Ma) overlapped with gold mineralization in the CTGF. Plutons of that particular age range are typically I-type, hornblende and biotite-bearing granodiorites and tonalites that make up 60% of the current exposure of the RAB. Late Carboniferous to Early Permian plutons (311 ± 3 to 283 ± 9 Ma) postdate the gold mineralization, crop out primarily in the eastern and southeastern portions of the RAB and account for only 6% of its units (Hutton and Rienks, 1997; Hutton et al., 1997).

2.2. Structural framework

2.2.1. Deformations prior to the emplacement of the Ravenswood Batholith

Metamorphic basement rocks in and adjacent to the RAB are often multiply deformed (Hutton and Rienks, 1997). However, little is known about their deformation history since a comprehensive structural analysis of the basement as a whole has not been attempted yet. Metamorphic basement units in the northern RAB are characterized by NW–SE (Charters Towers) to E–W (south of Charters Towers, Mingela) striking folds and axial cleavages (e.g. Peters, 1987b; Hutton et al., 1997). The Cambro-Ordovician basement (i.e. the Seventy Mile Range Group) in the southern RAB is dominated by N–S striking folds and E–W striking faults (Berry et al., 1992).

2.2.2. D_1: formation of E–W fabrics

The first deformation (D_1) to affect the RAB is preserved in Early to mid-Ordovician granitoids, coincided with a phase of limited intrusive activity and is thought to have occurred between mid-Ordovician and mid-Silurian times. D_1 was likely the result of NE–SW to N–S orientated regional shortening producing E–W striking shear zones with mylonitic fabrics being traceable over strike lengths up to 50 km and widths of 2 km. The most prominent of these high-strain zones is the anastomosing Alex Hill Shear Zone, which is characterized by a sinistral S–C fabric and a flat to gently E plunging S_1 mineral stretching lineation (Hutton and Rienks, 1997). Narrow, E–W striking mylonite zones in the Towers Hill Granite, such as those exposed in the Black Jack South, Black Jack PC and Stockholm pits, may have also formed during D_1. In addition, E–W to NW–SE striking mylonites with steeply plunging, possibly D_1 related stretching lineations were reported by Hutton et al. (1997), who interpreted these as thrust faults.

2.2.3. D_2: formation of NW–SE and NE–SW fabrics

The S_1 lineations in the western segment of the Alex Hill Shear Zone were possibly overprinted by NW–SE striking D_2 fabrics that are well developed in the northwestern portion of the RAB (Hutton and Rienks, 1997). In this area, S_2 fabrics preserved in narrow, NW–SE striking mylonite zones cutting the Towers Hill Granite suggest dextral shear senses. Similarly, fabric deflections and S–C fabrics preserved in the Weir Hill Shear Zone indicate a dextral sense of shear. The Weir Hill Shear Zone, a >5 km segment of the Burdekin River Lineament (cf. Heidecker, 1974), is also characterized by the shallow SE dip of its S_2 foliation (Hutton and Rienks, 1997). South of Mingela, an apparently sinistral NE–SW striking shear zone may also be related to D_2 as it cuts the E–W striking S_1 fabric of the Alex Hill Shear Zone. As a whole, these structures are believed to be

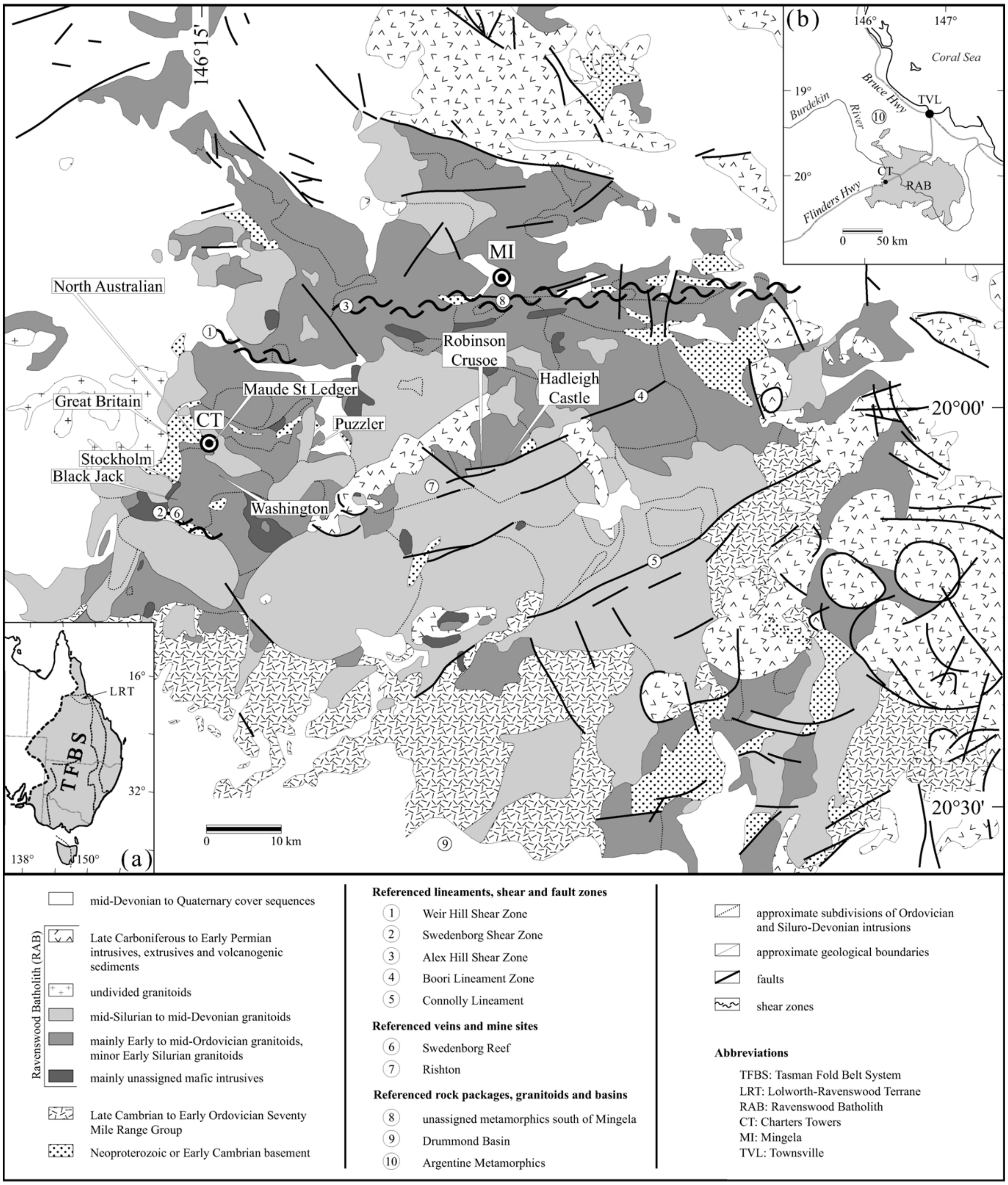

Fig. 1. Location of studied deposits and prospects in the Charters Towers Goldfield. The map also shows the major subdivisions of the Ravenswood Batholith, which forms part of the Lolworth–Ravenswood Terrane; modified after Hutton and Rienks (1997). Inset (a) illustrates the location of the Lolworth–Ravenswood Terrane within the Tasman Fold Belt System of eastern Australia; modified after Scheibner and Veevers (2000). Inset (b) shows the outcrop area of the Ravenswood Batholith; modified after Hutton and Rienks (1997).

the product of D_2 and linked to approximately N–S directed regional shortening sometime after D_1 and prior to the mid-Silurian (Hutton et al., 1997).

2.2.4. D_3: extension and granitoid emplacement into graben structures

Hutton and Rienks (1997) interpreted a number of mid-Silurian to mid-Devonian plutons with N–S to NE–SW striking axes of elongation as intrusions into graben. The authors linked the proposed graben formation to a Late Ordovician to Mid-Devonian extensional period (D_3), either related to broad doming of the RAB or directional extension along a N–S to NE–SW axis. However, the concept of Hutton and Rienks (1997) is poorly constrained as the precise ages of the concerned plutons are unknown and structural evidence for the graben model is not provided. Alternatively, the elongate plutons may have intruded shear or fault zones that were active during D_3, providing ascent paths for the magmas (e.g. Benn et al., 1998). Such a concept is in agreement with Tenison-Woods and Rienks (1992) who suggested that major lineaments, for example the <200-km-long, ENE–WSW striking Boori Lineament Zone and Connolly Lineament, controlled the emplacement of some mid-Silurian to mid-Devonian plutons.

Peters (1987b) proposed an extensional setting during the emplacement of mafic dykes at Charters Towers, permitting the injection of mantle-derived magma. The prominent NNW–SSE to N–S and NE–SW striking dyke swarms cut Early to mid-Ordovician granitoids but are truncated by Late Silurian to mid-Devonian intrusions (Peters, 1987b). Possibly synchronous mafic dyke swarms are known from other areas, such as NNE–SSW striking swarms in the southern portion of the RAB (Hutton and Rienks, 1997) and a NW–SE to E–W striking swarm at Hadleigh Castle.

In contrast to Hutton and Rienks (1997) but in agreement with Peters (1987b), D_3 was terminated during or prior to the Late Silurian. Such an age is constrained by the Late Silurian to Early Devonian timing of gold deposition, apparently coinciding with regional shortening. Given that even large tabular granites can be emplaced over geologically rapid times (<100 y to 1 my) without requiring unreasonably fast deformation rates in the underlying crust (Cruden, 1998), it may be possible that regional extension commenced significantly later than proposed by Hutton and Rienks (1997).

2.2.5. D_4: compression, brittle faulting and gold mineralization

Coinciding with Late Silurian to Early Devonian quartz vein formation and mineralization in the CTGF, the fourth deformation (D_4) was most likely one of regional shortening. D_4 was characterized by a mainly brittle deformation style and the reactivation of earlier structures. The postulated timing and nature of D_4 correspond well with the findings of other workers (e.g. Berry et al., 1992; Wellman, 1995; Hammond, 1986; Withnall and Lang, 1993).

2.2.6. Later brittle and ductile deformations

Later deformations were linked to (a) NE–SW directed extension and basin formation (e.g. Burdekin, Clarke River, Bundock Creek and Drummond Basins) from mid- to Late Devonian times (Henderson et al., 1998), and (b) possibly N–S to NNE–SSW directed shortening, resulting in the folding of mid-Devonian to Permian sedimentary and volcanogenic cover sequences about mainly E–W- to ESE–WNW-trending fold axes.

The effects of later deformations on the mapped intrusions and contained Siluro-Devonian vein systems were apparently minor. For example local segmentation of auriferous veins by strike-slip faulting on some levels at Hadleigh Castle Mine (Hampton, 2001, pers. comm.). Similar to Hadleigh Castle, minor reverse and normal separations of veins in the Washington and Robinson Crusoe Pits range between 0.1 and 1 m. Historic records (e.g. Reid, 1917) show several faults cutting the vein systems at Charters Towers. The largest of them, the 70°SE dipping Caledonia Fault (Fig. 3), gives a normal separation of 27 m to the workings in the Caledonia, Victory and Queen Mines.

2.2.7. Brief synthesis

Based on their work in the Seventy Mile Range, Berry et al. (1992) identified a Late Cambrian to mid-Ordovician cycle of basin formation and deformation. Repetitive cycles apparently occurred during (a) mid-Silurian granitoid emplacement into extensional crust and Late Silurian to Early Devonian gold mineralization during regional shortening, and (b) mid- to Late Devonian basin formation and later deformation (e.g. Berry et al., 1992; Henderson et al., 1998). At least some of these cycles may have been the result of inversions of the principal stresses, possibly controlled by continental scale tectonic forces. Table 1 presents a summary of the proposed deformations.

3. The character of the auriferous vein systems

3.1. Distribution, extent and continuity

In the CTGF the majority of auriferous vein systems are hosted by granites, granodiorites and tonalites of Early Ordovician to Late Silurian and possibly Early Devonian age. Only a small number of veins are wholly contained within metamorphic basement units or intrusions of dioritic to gabbroic composition. Their contribution to the total historic gold production was minor.

Auriferous vein systems at Charters Towers (Fig. 2) comprise shallow to moderately E, NW to NE and some rare S dipping veins (e.g. Moonstone Reef). Ore-shoots on the NW to NE dipping Brilliant (2.1 Moz Au), the N dipping

Table 1
Summary of the Lower to mid-Palaeozoic deformation history of the Ravenswood Batholith. Modified from Hutton et al. (1997). Key to abbreviations: CT: Charters Towers, HC: Hadleigh Castle, MI: Mingela

Deformation	Earlier D	D_1	D_2	D_3	D_4	Later D
Structure	Isoclinal folds; Axial cleavages	Shear zones; Mylonites; Thrusts	Shear zones; Mylonites; Fault zones	Faults and fault zones; Graben structures(?); Mafic and felsic dykes	Faults; Fault zones	Folds; Basins; Faults
Locality	CT, MI	CT, MI, southern RAB	CT, HC, MI	Faults: southern RAB; Graben: southern RAB; Dykes: RAB	CT, HC	Folds: northern and eastern RAB; Basins: RAB; Faults: CT, HC
Orientation	Fold axes: W to NW, SW; Axial cleavages: NW–SE to E–W	E–W, NW–SE	NW–SE, NE–SW to ENE–WSW(?)	Faults: NNE–SSW; Graben: N–S, NE–SW; Dykes: NNW–SSE to N-S, NE–SW, NNE–SSW	E–W to ENE–WSW, NNW–SSE to N–S, NW–SE	Folds: E–W to ESE–WNW, NW–SE, NE–SW; Faults: E–W, N–S, NNW–SSE, NE–SW to ENE–WSW
Comment	Multiple(?) deformations of the metamorphic basement	Apparently sinistral shear zones with shallow to steeply plunging mineral stretching lineations; episode of limited intrusive activity	Apparently sinistral and dextral shear zones and mylonites; episode of limited intrusive activity	Major intrusive episode	Major intrusive episode, brittle fracturing and faulting with minor displacement, gold mineralization	
Timing	Pre-Early Ordovician	Mid-Ordovician to mid-Silurian	Mid-Ordovician to mid-Silurian	Early to Late Silurian(?)	Late Silurian to Early Devonian	Post Early Devonian
Relation	Poorly known; earlier D structures cut by Early Ordovician intrusions	D_1 shear zones locally contain metamorphic basement slivers with earlier D fabrics	D_2 fabrics locally overprint E–W striking D_1 structures	Faults controlling granitoid emplacement; graben structures intruded by mid-Silurian to mid-Devonian granitoids; dykes cut Ordovician intrusives and are truncated by Late Silurian granitoids	Auriferous veins cut Silurian dykes and Early Ordovician to Late Silurian granitoids	Folding of mid-Devonian to Permian cover sequences; basin subsidence; local faulting and segmentation of auriferous veins by reverse, normal and strike-slip separation

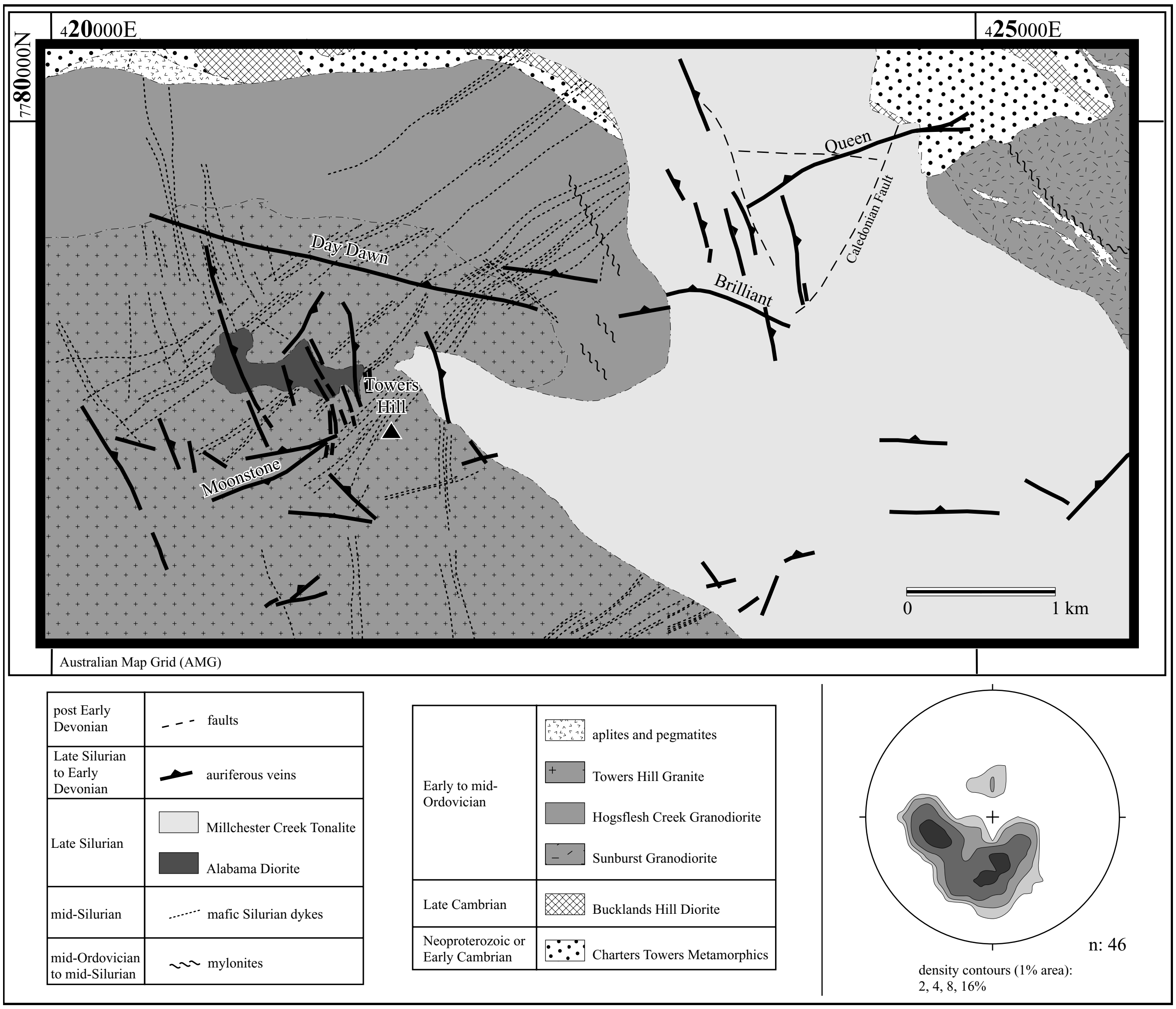

Fig. 2. Simplified geological map of the city of Charters Towers, also showing the main vein systems of the principle mining area; modified after Reid (1917), Peters (1987a,b) and Hutton and Rienks (1997). Inset: lower hemisphere, equal area projection illustrating the average orientation of historically mined reefs in the Charters Towers area; data obtained from Reid (1917).

Day Dawn (1.4 Moz Au) and the NW dipping Queen (180,000 oz Au) produced more than half of the gold extracted from the CTGF (Reid, 1917; Blatchford, 1953; Levingston, 1972; Peters, 1987b). These exceptional veins form an approximately E–W striking system of 5 km length. Furthermore, the Brilliant, Day Dawn and Queen Reefs are characterized by abundant splays, strike lengths of 1–2 km, vertical extents of 400–900 m and vein widths of up to 15 m. However, the majority of the auriferous veins in the Charters Towers area are 0.1–1 km long. Average vein widths are 1 m or less, whereas vertical extents are generally <400 m (Reid, 1917).

Structurally and mineralogically similar veins in the Hadleigh Castle area are found along the ENE–WSW striking 'Rishton–Hadleigh Castle Corridor' (Fig. 3a) that coincides with a >10 km segment of the Boori Lineament Zone. At Hadleigh Castle, the 01 Lode is hosted within a moderately SSE dipping segment of the lineament zone and accompanied by further mineralized SE to SW dipping structures in its hanging wall (Fig. 3b and c). The southerly dip of the vein system (Fig. 3d) distinguishes it from the orientation of veins in the Charters Towers area, although a small number of S dipping veins are also present at Charters Towers. In contrast to Charters Towers, auriferous veins at Hadleigh Castle are spatially associated with earlier tourmaline veins. The latter dip shallow to moderately E to SE and SW and are hosted by the Hangingwall Granodiorite (corresponds to the Boatswain Granodiorite of Hutton and Rienks, 1997). According to Hodkinson (1998), mining at Hadleigh Castle yielded >125,000 oz Au extracted from a zone having a strike length of 250 m, an apparent width of up to 80 m and a vertical dimension of

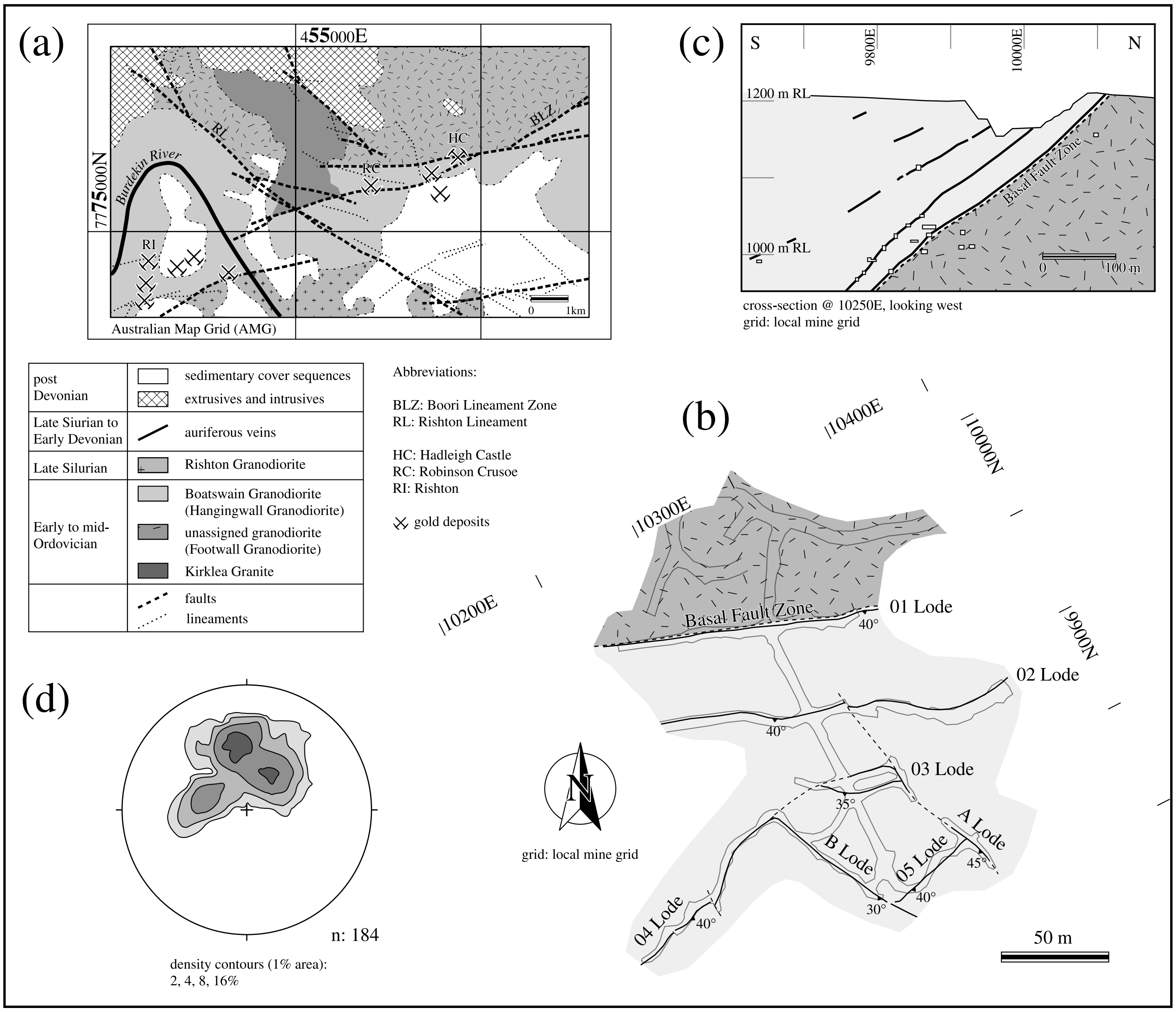

Fig. 3. (a) Simplified geology of the Hadleigh Castle area, also showing principle faults, lineaments and gold deposits; modified after Rienks et al. (1996). Gold deposits are clustered along the ENE–WSW-trending 'Rishton–Hadleigh Castle Corridor' coinciding with the Boori Lineament Zone. (b) Geological sketch map of the 1110 m RL, Hadleigh Castle Mine; modified after Hodkinson (1998). (c) Cross-section of the deposit illustrating undulation, continuity and shallow to moderate S dip of the vein system; modified after Hodkinson (1998). (d) Lower hemisphere, equal area projection showing the orientation of auriferous veins.

400 m. Individual veins, however, may only reach 50 m along strike and do not exceed a maximum thickness of 1 m. A brief summary of the orientations and timing of the studied veins is provided in Table 2.

3.2. Vein geometries and intersections

Vein geometries are relatively uniform with most veins across the study area showing at least some of the following characteristics: (a) undulations in strike and/or dip, (b) average dips in the order of 25–45°, (c) pinching and swelling, (d) thickening or thinning at vein/fault or vein/vein intersections, and (e) ore deposition in shallower dipping vein portions (Fig. 4). Exposures in the Hadleigh Castle Mine provided the rare opportunity to examine vein intersections, namely those of the 01$\frac{1}{2}$ and 02 and of the B and 05 Lodes. As illustrated by Fig. 5, intersecting veins do not appear to displace each other. Near the actual intersection the veins pinch out or change their strikes and/or dips.

3.3. Mineralogy, vein textures and wallrock alteration

Auriferous quartz veins from the Charters Towers and Hadleigh Castle areas have a relatively similar and simple mineralogy and paragenesis. High-grade vein portions generally comprise at least two quartz generations, sulfides (the most common being pyrite, galena and sphalerite), sericitized wallrock fragments and late calcite phases. Gold is intimately associated with the sulfides and precipitated as

Table 2
Summary of the orientations of the studied auriferous veins. The strikes and dips of the Maude St Ledger, North Australian and Great Britain Reefs are average orientations based on Reid (1917) and Levingston (1972). Key to abbreviations: CT: Charters Towers, HC: Hadleigh Castle

Area	Studied deposits		Vein types	Strike	Dip	Timing
CT	Maude St Ledger		Quartz–sulfide veins	340°;	5–50°ENE;	Pb isotope model age: 400 Ma (Carr et al., 1988);
	North Australian			350°;	25°ENE;	$^{40}Ar/^{39}Ar$ age: 414.8 ± 1 Ma (Perkins and Kennedy, 1998);
	Great Britain			290–310°	20–40°NNE to NE	K–Ar age: 416–397 ± 4 Ma (Morrison et al., unpubl. data)
	Washington/Golden Alexandra		Quartz–sulfide veins;	065–115°;	5–65°NNE to NNW	
			Stockwork veins			
	Stockholm			070–085°	10–75°N to NNW	
	Newtown Butler, Black Jack PC,			270–300°;	5–80°WNW to E	
	Black Jack South			330–350°, 010°;		
				030–060°;		
				080–090°		
HC	Hadleigh Castle Lode System	01 Lode;	Quartz–sulfide veins	060–095°	25–60°S to SSE	Pb isotope model age: 380 Ma (Carr et al., 1988);
		02 Lode;				$^{40}Ar/^{39}Ar$ age: 412.2 ± 2.4 to 400.1 ± 4.9 Ma (Kreuzer, unpubl. data)
		04 Lode		350°, 050–060°;	5–55°E to SE;	
				075–080°;		
				090–100°;		
		05 Lode;		050°;	40°SE;	
		B Lode		100–150°	15–50°SSW to SW	
	Robinson Crusoe		Quartz–sulfide veins;	350–020°;	8–75°E to S	
			Stockwork veins	045–065°;		
				075–095°		

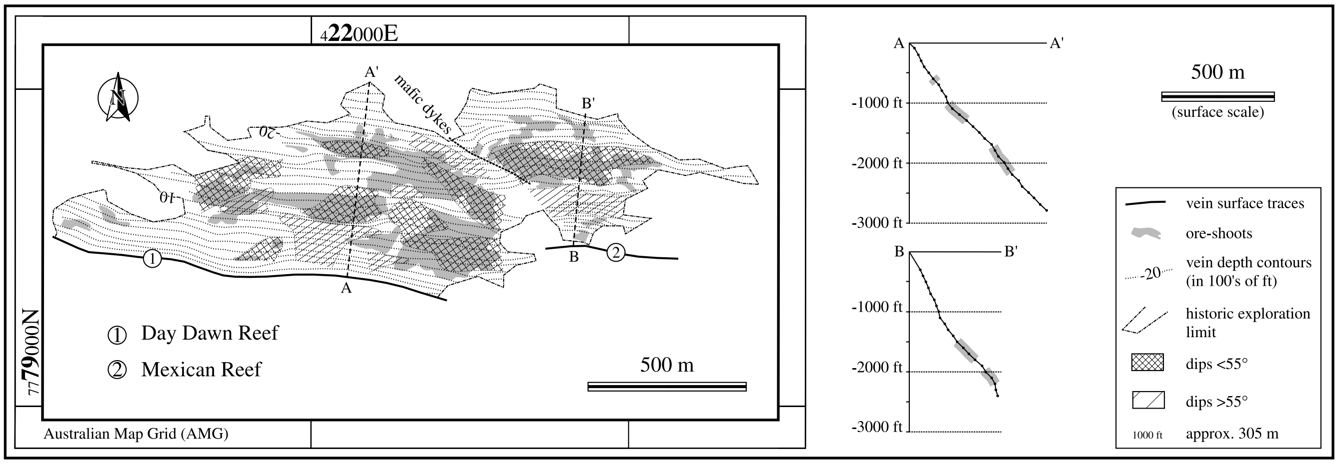

Fig. 4. Vein contour map of the Day Dawn and Mexican Reefs, also illustrating the historically mined orebodies. Vein depth contours were likely derived from plans and cross-sections of the historic workings; modified after Levingston (1972). Ore deposition occurred preferentially in shallower dipping vein segments (<55°) of the Day Dawn and Mexican Reefs; modified after Peters (1987b). Presented cross-sections are based on the vein depth contour maps.

10–200-μm-wide grains in fractures, vugs and defects of paragenetically earlier quartz and sulfides, while coarser (up to 2 mm wide) gold grains occur at quartz/sulfide and sulfide/sulfide grain boundaries.

Barren vein segments are characterized by buck textures, namely mutually interlocking, subhedral to euhedral quartz grains. Sulfide-rich and thus potentially gold-rich portions, in contrast, comprise at least one, but generally a combination of the following additional textures: (a) ribbon textures defined by enclosed wallrock slivers, or bands of gray quartz and sulfides alternating with white buck quartz, (b) isolated and interconnected comb textures with euhedral quartz crystals, typically occurring in shallow dipping vein segments, (c) aggregate breccia textures (e.g. Dowling and Morrison, 1989) consisting of comb and buck quartz modified by deformation, resorption and subgrain development, and (d) stylolite textures with sawtooth-shaped cross-sections that are subparallel to the vein margins and apparently more abundant in vein segments devoid of comb quartz. Macro- and microscopical observations indicate that vein segments with comb or aggregate breccia textures host the bulk of the ore minerals and that these particular vein portions were the preferred sites of gold deposition.

Intimately linked to the auriferous veins are narrow, zoned alteration halos (Peters, 1987b) that envelope the veins (Fig. 6) and are absent from structures that did not permit the flow of gold-bearing fluids. Proximal to the auriferous veins, sericitic hydrothermal alteration zones typically comprise carbonate phases, disseminated pyrite and abundant sericite replacing all primary constituents of the granitic wallrocks except for quartz. The distal alteration zone is always wider than the proximal halo and is characterized by a propylitic mineral assemblage and reddened feldspars (cf. Cassidy and Bennet, 1993). Commonly, the alteration halos reach two to three times the widths of the veins they accompany (e.g. Hartley and Dash, 1993). Identical but narrower zoned alteration envelopes are evident from barren structures whose orientations are similar to those of the auriferous veins. However, most of these barren structures are either structures linking mineralized vein segments or splay terminations that did not dilate sufficiently for mineral deposition to occur. The zoned wallrock alteration is intimately associated with the auriferous veins and linked fracture network, thus providing a reliable criterion for assessing whether a fracture was part of the hydrothermal system or not.

3.4. Geochemical characteristics

Fluid inclusion analyses of vein samples from the Brilliant, Day Dawn and Queen Reefs indicate low to moderate salinity (5.3–11 wt% NaCl equiv.), water-rich ore fluids with a depositional temperature range of 240–300 °C and low, variable CO_2 contents (Peters and Golding, 1989).

3.5. Depth of formation

Based on the character of the mineralized faults and their gouge, Peters and Golding (1989) estimated a depth of quartz vein formation and gold deposition ranging from 2.5 to 3.5 km (0.75–1.05 kbar). The model of Peters and Golding (1989) implies that mid-Silurian to mid-Devonian granitoid emplacement occurred at similar crustal levels. However, spatially and temporally associated volcanics and sediments, typical for high-level environments, are lacking (e.g. Hutton and Rienks, 1997). Furthermore, the mainly greenschist or higher-grade facies metamorphic basement rocks suggest that both intrusions and vein systems formed at depths of at least 5 km (2 kbar). Such an environment seems more reasonable given the mesothermal temperature range of the ore-bearing fluids (cf. Baker, 2003).

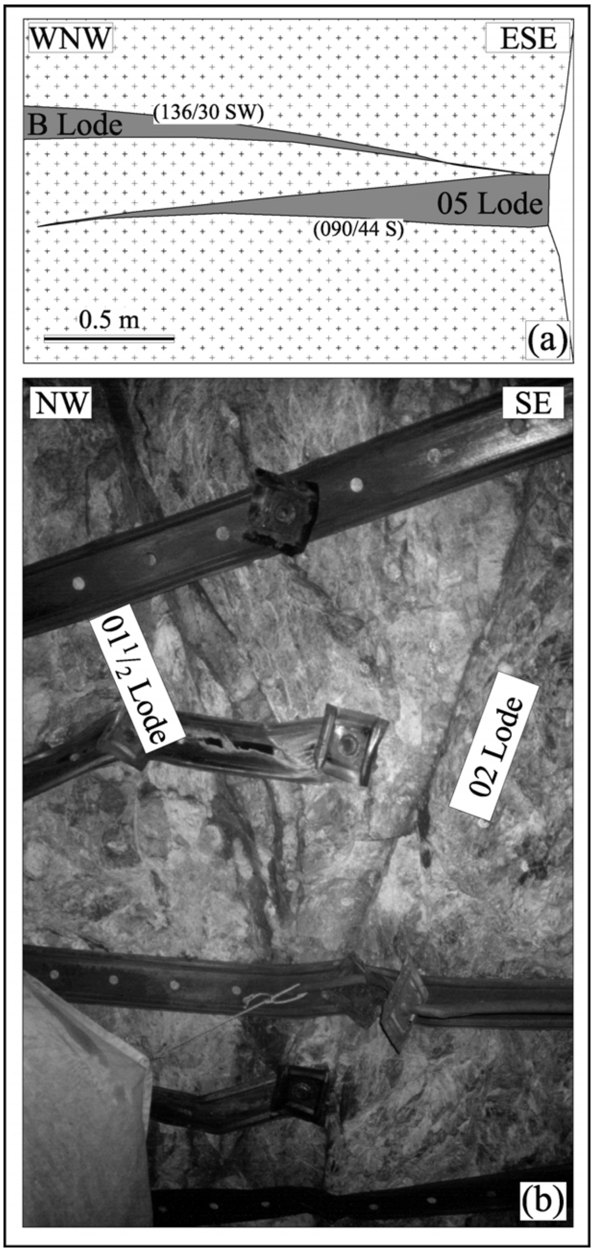

Fig. 5. Vein intersections at Hadleigh Castle Mine. (a) Intersection of the B and 05 lodes on 1090 m RL. The 05 Lode swells towards the east while the B Lode—here at its eastern end—pinches to a barren fracture when intersecting the 05 Lode. (b) Intersection of the 01 $\frac{1}{2}$ and 02 Lodes, exposed in the roof along a drive on 855 m RL. Note the horsetail splays on the 01 $\frac{1}{2}$ Lode near the intersection. Field of view approximately 10 m, looking northeast; photograph kindly provided by Andrew Allibone.

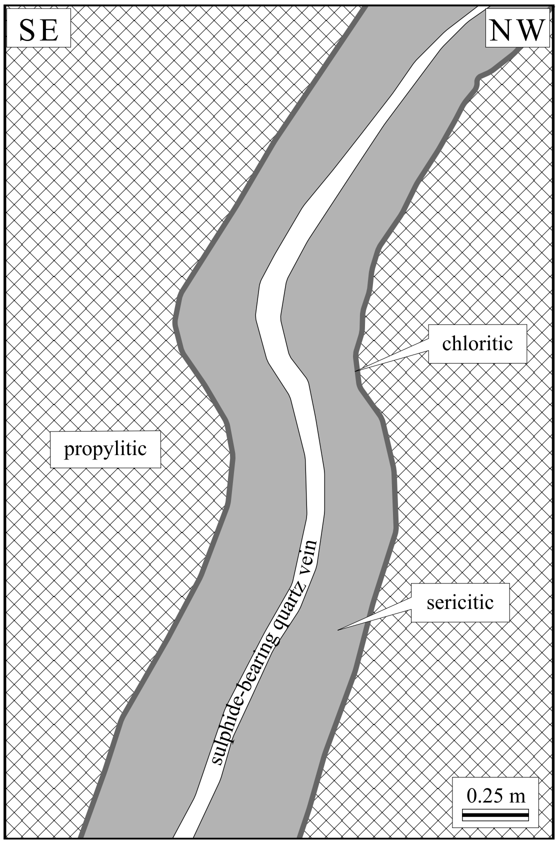

Fig. 6. Sketch of a sulfide-bearing quartz vein in the Robinson Crusoe Pit. Accompanied by symmetrically zoned wallrock alteration. The envelope consists of a narrow zone of sericitic alteration that forms part of a broader, propylitic halo around the vein. The boundary between the serticitic and propylitic zones is marked by a narrow chloritic alteration front.

3.6. Age of mineralization

The K–Ar dating of alteration sericite from granitic wallrocks of the Day Dawn and Brilliant Reefs provided a range of potential mineralization ages from 416 to 397 ± 4 Ma (Morrison et al., unpubl. data). Subsequent $^{40}Ar/^{39}Ar$ dating of alteration sericite from the Brilliant Reef indicated a potential 414.8 ± 1 Ma age (Perkins and Kennedy, 1998) for gold mineralization at Charters Towers. Lead isotope modeling by Carr et al. (1988) on the other hand suggested a mineralization age of 400 Ma for vein systems at Charters Towers and 380 Ma for the Hadleigh Castle deposit (Carr et al., 1988). Recent $^{40}Ar/^{39}Ar$ dating of hydrothermal sericite grains from granitic wallrocks of the 04 Lode at Hadleigh Castle provided potential mineralization ages ranging from 412.2 ± 2.4 to 400.1 ± 4.9 Ma (Kreuzer, un-publ. data). In addition to the overlapping radiometric ages, the similarity of vein mineralogy, ore mineral paragenesis and alteration assemblage implies that gold mineralization at Charters Towers and Hadleigh Castle occurred contemporaneously.

4. Key points from deposit studies

4.1. Central Decline (Maude St Ledger Reef)

The studied segment of the Maude St Ledger Reef (Figs. 7 and 8) is lenticular with the (stoped) orebody being confined to a 5–30°E to ENE dipping, up to 1 m wide vein section. Surrounding vein portions are barren, dip 30–50°E to NE and are < 0.2 m wide. In cross-section, the geometry

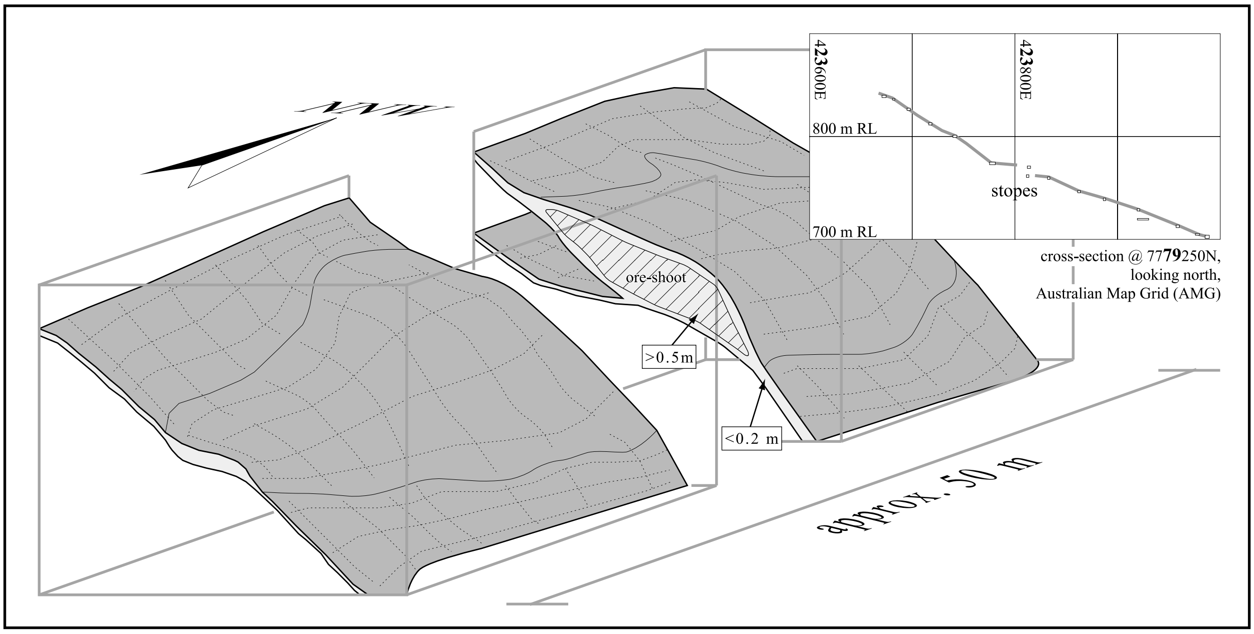

Fig. 7. Schematic block diagram of the studied segment of the Maude St Ledger Reef, illustrating how the (stoped) ore-shoot is confined to a shallow dipping, lenticular, and apparently dilatant vein segment. Inset: cross-section of the same segment, showing significant flattening of the host structure where the stopes are situated; SURPAC-based section kindly provided by Charters Towers Gold Mines staff.

of the studied vein segment resembles that of dilational jogs in shortening regimes (cf. fig. 14d in Cox et al., 2001). The (stoped) orebody appears to coincide not only with a right hand bend but also a flattening of the vein structure. As illustrated in Fig. 8, barren vein sections deviate from the mean NNW–SSE strike of the vein segment that hosts the (stoped) orebody.

Two wear groove striations in the hanging wall of the Maude St Ledger Reef plunge 15–25°ENE to ESE indicating dip-slip movement along the host fault. The wear groove striations (and those observed at the localities listed below) possibly formed by asperity ploughing, also known as abrasive wear (e.g. Blenkinsop, 2000). Their timing cannot be determined beyond doubt, however the 426 ± 4 Ma (Hutton and Rienks, 1997) age of the striated Millchester Creek Tonalite provides a Late Silurian maximum age. Furthermore, evidence for post-D_4 fault reactivation is lacking. Hence, the observed wear groove striations possibly formed during Late Silurian to Early Devonian times and thus linked to the same tectonic regime as gold mineralization.

4.2. Washington Pit (Golden Alexandra Reef)

The (stoped) 20°NE dipping (Levingston, 1972) Golden Alexandra Reef is accompanied by a stockwork of principally 6–46°N to NE dipping quartz–sulfide veins (Fig. 8). The occurrence of subhorizontal veins suggests vein formation linked to shortening rather than extension. In addition, a stockwork vein in the northwestern corner of the open pit cuts an earlier aplite, displacing the dike in an apparently reverse sense.

Wear groove striations on the upper surface of a NE dipping stockwork vein plunge 42–45°ENE, indicating highly oblique dip-slip on this particular vein surface and possible oblique movement on the stockwork as a whole. Since the striations are carved into a stockwork vein, their potential maximum age is Late Silurian. No evidence could be found for later movement along the fissures hosting the stockwork veins, implying the wear groove striations may have formed during the same tectonic regime as gold deposition. If so, movement along N to NE dipping fractures may not have been entirely reverse but reverse sinistral.

4.3. Black Jack South Pit (Black Jack Reef)

The Black Jack South Pit worked the near-surface extension of the 30°E dipping (Levingston, 1972) Black Jack Reef. It shows that (a) the main vein, like the Golden Alexandra Reef, is accompanied by a stockwork of narrow quartz–sulfide veins (Fig. 8), (b) zoned alteration envelopes and sulfide-bearing quartz veins in the pit walls are mainly confined to E to NE and N dipping structures, (c) an earlier shear zone and an accompanying aplite are separated in a reverse sense by a N dipping fault in the western pit face, and (d) an ENE dipping zone of cataclasite in the northern pit face also recorded apparent reverse movement as implied by a number of horizontal quartz veins contained within the cataclasite.

Apparent reverse movement on both N and ENE dipping structures may be explained with a NNE–SSW to ENE–WSW orientation of the shortening axis during quartz vein formation and gold deposition. As a consequence, E dipping faults may have experienced reverse dextral and N dipping

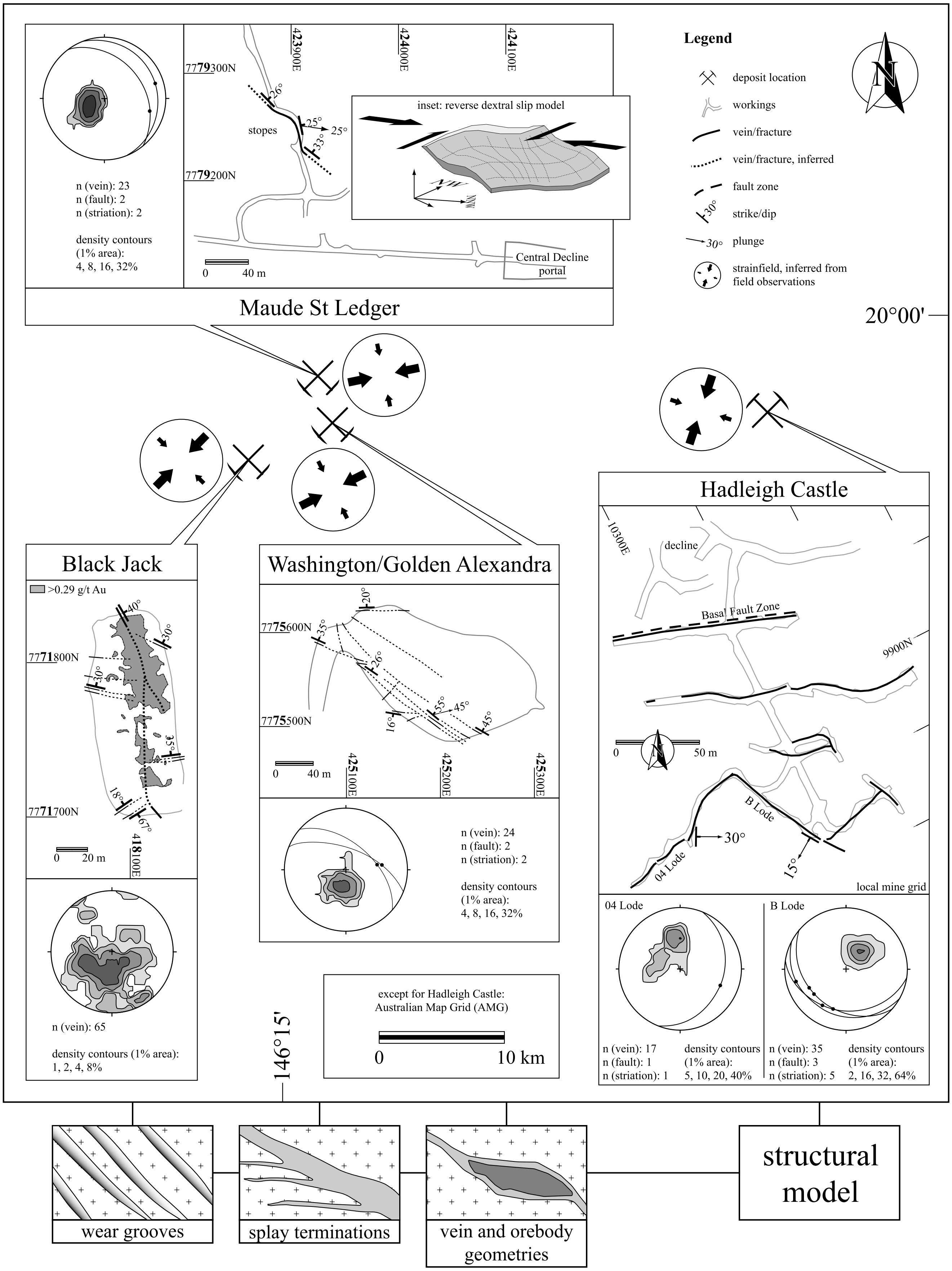
Maude St Ledger
n (vein): 23
n (fault): 2
n (striation): 2
density contours
(1% area):
4, 8, 16, 32%
7779300N
7779200N
423900E
424000E
424100E
stopes
inset: reverse dextral slip model
Central Decline
portal
0 40 m
Legend
deposit location
workings
vein/fracture
vein/fracture, inferred
fault zone
strike/dip
plunge
strainfield, inferred from
field observations
20°00'
Black Jack
>0.29 g/t Au
7771800N
7771700N
418100E
0 20 m
n (vein): 65
density contours (1% area):
1, 2, 4, 8%
Washington/Golden Alexandra
7775600N
7775500N
425100E
425200E
425300E
0 40 m
n (vein): 24
n (fault): 2
n (striation): 2
density contours
(1% area):
4, 8, 16, 32%
Hadleigh Castle
10300E
decline
Basal Fault Zone
9900N
0 50 m
B Lode
04 Lode
local mine grid
04 Lode
B Lode
n (vein): 17
n (fault): 1
n (striation): 1
density contours
(1% area):
5, 10, 20, 40%
n (vein): 35
n (fault): 3
n (striation): 5
density contours
(1% area):
2, 16, 32, 64%
except for Hadleigh Castle:
Australian Map Grid (AMG)
0 10 km
146°15'
wear grooves
splay terminations
vein and orebody
geometries
structural
model

faults reverse sinistral slip. Such a model would agree with the contoured geometry of the Black Jack South orebody (Fig. 8). The N–S striking ore-shoot appears to be confined to a right bend in the host structure terminating against the ENE dipping cataclasite at its northern and against a NE dipping fracture at its southern end.

4.4. Hadleigh Castle Mine (Hadleigh Castle Vein System)

Below and above the stopes (1130–1090 m RL), the SW dipping B Lode (Fig. 8) is poorly mineralized, narrower and steeper dipping (Hodkinson, 2001, pers. comm.). Like the Maude St Ledger Reef at Charters Towers, the geometry of the studied vein segment resembles that of dilational jogs in shortening regimes. The timing of 7–15°SW to WSW plunging wear groove striations in the hanging wall of the B Lode (1110 m RL) is poorly constrained. However, given that the wear groove striations possibly recorded the last fault-slip event and evidence for post-D_4 movement along the host fracture is lacking, it appears likely that the wear groove striations formed during the same tectonic regime as gold mineralization.

The 20–55°S to E dipping 04 Lode (Fig. 8) is characterized by numerous subhorizontal to shallow dipping diverging splays and splay terminations. At the western end of 920 m RL, for instance, the 04 Lode forms a 0.7-m-wide dilational jog with several 5–7°SW dipping splay terminations accompanied by isolated flat-lying quartz–sulfide veins (Fig. 9). The vein geometries and subhorizontal to shallow dipping splay terminations are supportive of a concept of quartz vein formation in a shortening regime. Wear groove striations in the hanging wall of a 30°ESE dipping segment of the 04 Lode (920 m RL) plunge 30°ESE. Like the striations associated with the B Lode and based on the same criteria, the wear groove striations in the hanging wall of the 04 Lode are thought to have formed during D_4, that is during the same tectonic regime as gold mineralization.

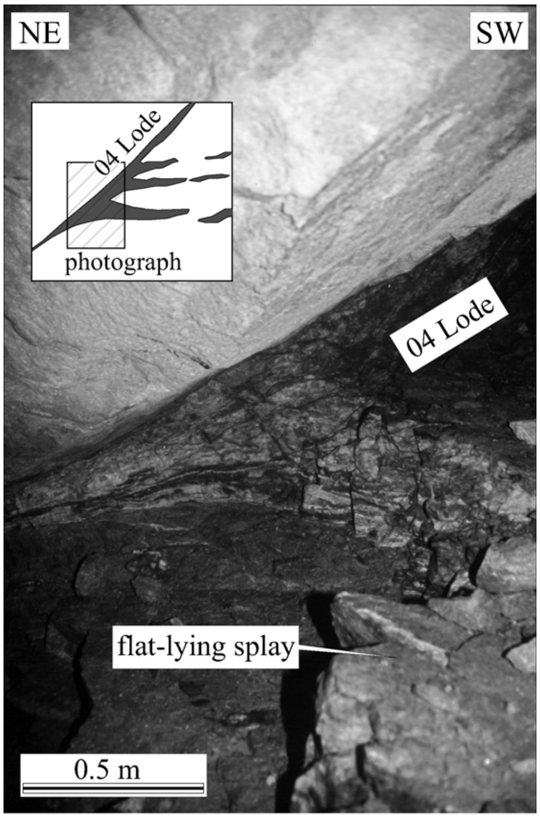

Fig. 9. A flat-lying splay termination branching off the 04 Lode, 920 m RL. Dark bands within the auriferous vein contain abundant fragments of earlier tourmaline veins; photograph kindly provided by Andrew Allibone. Inset: sketch illustrating the occurrence of additional splays and isolated veins near the splay termination.

5. Systematic orebody classification

A comprehensive outline of the principles and applications of systematic orebody classification using so-called shape graphs can be found in Blenkinsop (2004, this volume). Here, the method of Blenkinsop (2004, this volume) has been applied to characterize and compare the studied orebodies, as well as some of the historically mined ore-shoots. Literature data and plans and cross-sections of the historic workings (e.g. Reid, 1917; Levingston, 1972; Hartley and Dash, 1993; Hartley, 1996) were used to obtain the *U*, *V* and *W* axes for a selection of historically mined ore-shoots with well known dimensions. The axes of many studied orebodies on the other hand were difficult to evaluate, especially since some ore-shoots (e.g. at Hadleigh Castle) are currently open at depth. At the same time, the actual dimensions of recently mined orebodies are often poorly defined (e.g. Black Jack, Stockholm, Washington, Robinson Crusoe). For the latter, the extent of remaining stockwork veins was used to define an overall (uneconomic) mineralized zone, which essentially envelope the stoped (economic) vein portions. Additional issues that may have biased some results towards lower *U*/*V* and higher *V*/*W* ratios, respectively, concern the fact that the actual width of the historic orebodies is not always known in detail. However, width averages and ranges are available (e.g. Reid, 1917; Levingston, 1972). Secondly, different cut-off grades and mining methods of present and historic operations may have contributed to ellipsoids defined by different cut-off grades.

With these potential shortcomings in mind, the CTGF data was plotted on a shape graph (Fig. 10) revealing four distinct populations whose characteristics are summarized

Fig. 8. Key points from the deposit studies forming the basis of the structural model. The proposed NNE–SSW to ENE–WNW directed strainfield is based on the orientations of auriferous veins, wear groove striations, and reverse separations. Accompanying projections are lower hemisphere, equal area projections.

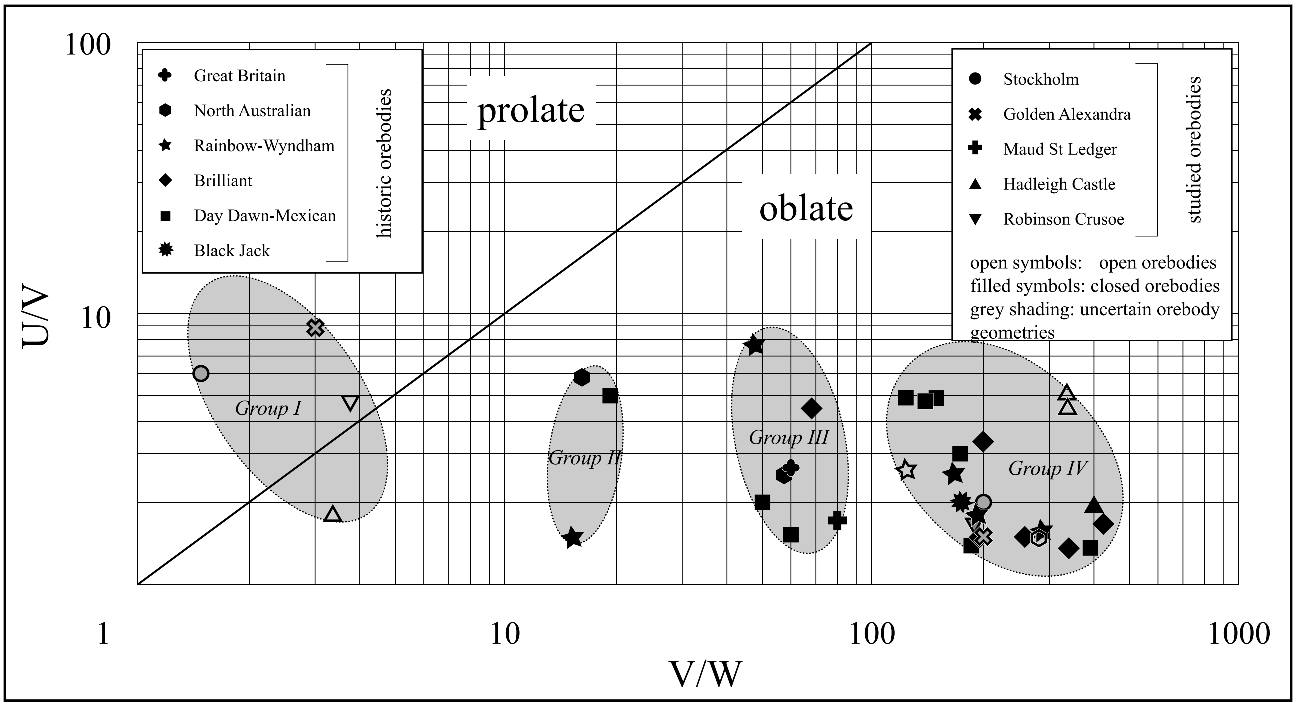

Fig. 10. Shape graph (cf. Blenkinsop, 2004, this volume) illustrating four distinct orebody populations indicated by shaded ovals.

in Table 3. Due to their uncertain boundaries, the axes of most Group I orebodies (Golden Alexandra, Stockholm and Robinson Crusoe) had to be approximated by the extent of stockwork veins enveloping the stoped ore-shoots. In contrast to all other data, these orebodies plot in the prolate field ($1 < j < \infty$). Also included in Group I, but plotting in the oblate field, is the data point representing the entire productive zone of the vein system at Hadleigh Castle. Its shape is thought to be a result of the orebody being presently open at depth. If the productive zone would prove to continue further down dip, the *U*/*V* ratio of the orebody would be expected to shift upwards, and thus to plot in the prolate field. Taken as a whole, Group I discriminates tubular or potentially tubular zones of high fracture density.

Groups II–IV are characterized by three distinct data clusters, progressively decreasing *j* values and oblate orebody shapes ($0 < j < 1$). Given that veins are generally narrow and hosted by planar deformation zones, it is not surprising that the tabular ore-shoots of Groups II–IV are dominated by single short axes (*W*). Group IV orebodies have the lowest *j* values and *V*/*W* ratios and comprise some of the largest and richest ore-shoots in the CTGF, for example the main Brilliant (averaging up to 105 g/t Au) and Mexican (averaging up to 46 g/t Au) orebodies. However, Group IV also includes sulfide-bearing stockwork veins, such as those accompanying the Golden Alexandra and Stockholm Reefs, and the Robinson Crusoe Lode. The economically insignificant stockwork veins are clearly dominated by their narrow *W* axes (< 10 cm). Overall, the most productive orebodies are characterized by widths > 10 cm and ratios of $U/V < 5$ and $V/W > 50$.

6. Indications of reactivation

6.1. Reactivation of pre-existing planes of weakness

D_1 to D_3 as well as deformations prior to the emplacement of the RAB produced structures (e.g. fold axes, axial cleavages, foliations, and fractures) that coincide with the principal orientations of auriferous veins in the Charters Towers and Hadleigh Castle areas (Table 4). Some of the pre-D_4 discontinuities are known to have been reactivated during D_4 as a number of veins and ore-shoots are wholly or partially hosted in these earlier structures. The most prominent example from Charters Towers is the Day Dawn Reef, an unusually steep dipping (45–65°N) vein that, over much of its course, followed and partially replaced an older E–W striking mafic dyke (Reid, 1917; Levingston, 1972). At Hadleigh Castle, the 01 Lode is hosted within a segment of the Boori Lineament Zone. The pre-existing discontinuity (cf. Hutton and Rienks, 1997) was apparently reactivated during D_4, thus becoming the site of local quartz vein formation and gold mineralization. Tourmaline veins predating gold mineralization are most abundant in the vicinity of the 02, 04 and B Lodes. These auriferous veins also contain ubiquitous tourmaline vein fragments, and are, in the case of the B Lode, partially hosted in fractures accommodating the earlier tourmaline veins (Fig. 11). Therefore, these earlier structures provided significant loci for quartz vein formation and many tourmaline veins may have been partially or wholly reworked during vein growth. Throughout the CTGF, auriferous veins follow geological contacts or are hosted

Table 3
Summary of orebody populations obtained using a so-called shape graph (cf. Blenkinsop, 2004, this volume). Key to abbreviations: (s): strike length, (d): dip extent, (w): width of plotted orebodies

	Group I	Group II	Group III	Group IV
k values	0.5–4.8	0.07–0.39	0.02–0.16	0.003–0.043
Geometries	Mainly prolate	Oblate	Oblate	Oblate
Dimensions	U(s) > V(d) > W(w); U(d) > V(s) > W(w)	U(s) > V(d) > W(w); U(d) > V(s) > W(w)	U(s) > V(d) ≫ W(w); U(d) > V(s) ≫ W(w)	U(s) > V(d) ≫ W(w); U(d) > V(s) ≫ W(w)
Length of U axes[a]	150–400 m	30–100 m	60–170 m	50–800 m
Dominant orebody plunges[a]	No data	N and E	NW to NE, and E	NW to NE, SW to SE, and E
Orientation of U axes with respect to σ_1	Stockholm: U(s) parallel to oblique to σ_1; Golden Alexandra: U(s) perpendicular to oblique to σ_1; Robinson Crusoe: U(s) parallel to oblique to σ_1; Hadleigh Castle Vein System: U(d) perpendicular to oblique to σ_1	Great Britain: U(d) parallel to oblique to σ_1; North Australian: U(s) and U(d) ore-shoots perpendicular to oblique to σ_1; Rainbow–Wydham: U(s) and U(d) ore-shoots perpendicular to oblique to σ_1; Brilliant: U(d) parallel to oblique to σ_1; Day Dawn–Mexican: U(s) and U(d) ore-shoots perpendicular to oblique to σ_1; Black Jack: U(s) perpendicular to oblique to σ_1; Maud St Ledger: U(s) perpendicular to oblique to σ_1; Hadleigh Castle (individual orebodies): U(s) and U(d) ore-shoots perpendicular to oblique to σ_1		
Comments	Vein systems consisting of a number of parallel veins separated by barren host rock; zones of closely spaced stockwork veins enveloping stoped orebodies	Closed, small to medium-sized ore-shoots; these accompany larger orebodies hosted within the same vein structures	Closed, medium-sized ore-shoots and distinct domains of larger ore-shoots	Medium-sized to very large ore-shoots and individual stockwork veins; boundaries open, closed or uncertain

[a] Data obtained from Reid (1917) and Levingston (1972).

Table 4
Comparison of the orientation of pre-D_4 structures and the auriferous veins, which formed during D_4. Key to abbreviations: CT: Charters Towers, HC: Hadleigh Castle

Strike	Timing	Structural elements	Area	Corresponding veins/ore-shoots
NW–SE	Pre-D_1	Folds and axial cleavages in the Charters Towers Metamorphics[a]	CT	Veins in metamorphic host rocks (e.g. Great Britain Reef)[b]
	D_3	Felsic dyke swarm	CT	Veins south of Black Jack[b]
	D_1–D_2	Mylonites and shear zones[a]	CT	Ore-shoots of the Swedenborg Reef[b]
	Early D_4(?)	Tourmaline veins	HC	B Lode
NNW–SSE to N–S	D_3	Mafic dyke swarm	CT	Veins around Towers Hill (e.g. North Australian Reef)[b]
	D_1–D_3(?)	Stockholm Fault Zone	CT	Stockholm Reef
	D_1–D_3(?)	Western Fault	HC	Veins on 965 Level (Hadleigh Castle)[c]
E–W to ENE–WSW	D_3	Mafic dyke swarm[b]	CT	Day Dawn Reef[b]
	D_1	Mosgardies Shear Zone[a]	CT	Veins south of the Brilliant Reef[b]
	D_1–D_3(?)	Boori Lineament Zone[b]	HC	Main Lode System
	Early D_4(?)	Tourmaline veins	HC	02 Lode
NE–SW	D_3	Mafic dyke swarm	CT	Veins around Towers Hill (e.g. Moonstone Reef)[b]
	Early D_4(?)	Tourmaline veins	HC	04 Lode

[a] Data obtained from Hutton and Rienks (1997).
[b] Data obtained from Reid (1917) and Levingston (1972).
[c] Data obtained from Hodkinson (2001, pers. comm.).

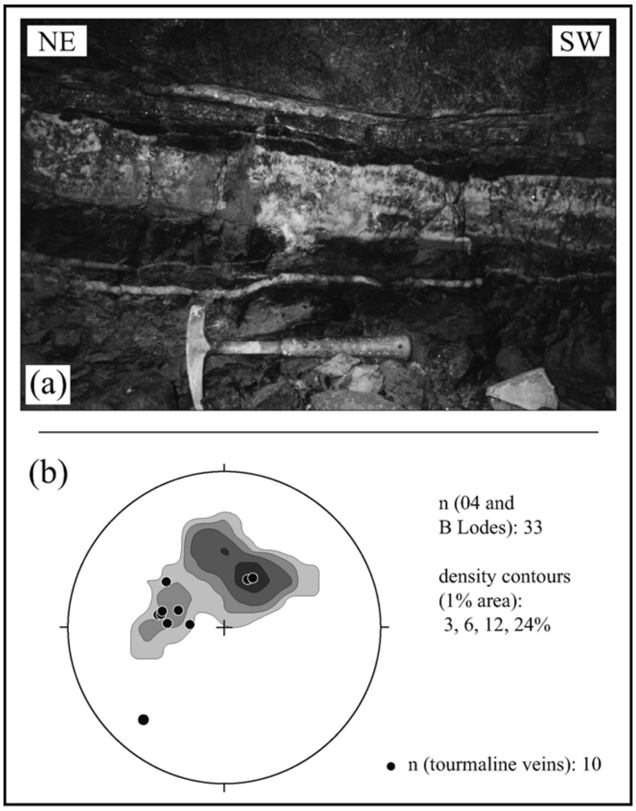

Fig. 11. (a) An example of fault reactivation from the B Lode, 1110 m RL. The host structure contains an older tourmaline vein (black) that was cracked open and injected by later quartz (white) and sulfides linked with the gold mineralization; photograph kindly provided by Andrew Allibone. (b) Lower hemisphere, equal area projection illustrating the corresponding orientations of tourmaline veins (poles) and the 04 and B Lodes (contoured poles).

within earlier joints and faults, thus providing further evidence that reactivation of suitably orientated structures was a widespread phenomenon during D_4.

6.2. Repeated movement on vein structures

Evidence for repeated movement on host faults during D_4 comes from both Charters Towers and Hadleigh Castle. The Maude St Ledger Reef, for instance, recorded at least two such events. Locally, the upper 20–50 cm of the vein comprise angular to weakly rounded, monomict breccia clasts. These are 0.1–7-cm-wide, consisting of primary white buck quartz cut by sheeted calcite veins. Clast rotation appears to have been minimal as sheeted calcite veins, which are absent from the gray matrix quartz, have approximately similar orientations across the cemented fragments (Fig. 12). Brecciation postdated a prominent episode of sheeted calcite veining and, because these calcite veins cut pyrite, sphalerite and galena, paragenetically earlier sulfide deposition. However, the gray matrix quartz hosts paragenetically later pyrite, sphalerite, galena and, most importantly, gold. Brecciation may have been related to a sudden opening of space caused by rapid fault slip and probably linked to a temporal variation in fluid pressure prior to gold deposition. According to the criteria of Jebrak (1997), brecciation may have been the product of hydraulic or critical fracturing. Both processes are fluid-assisted, typically follow pre-existing planes of discontinuity, and generate angular fragments and fragmentation textures without significant clast rotation (Jebrak, 1997).

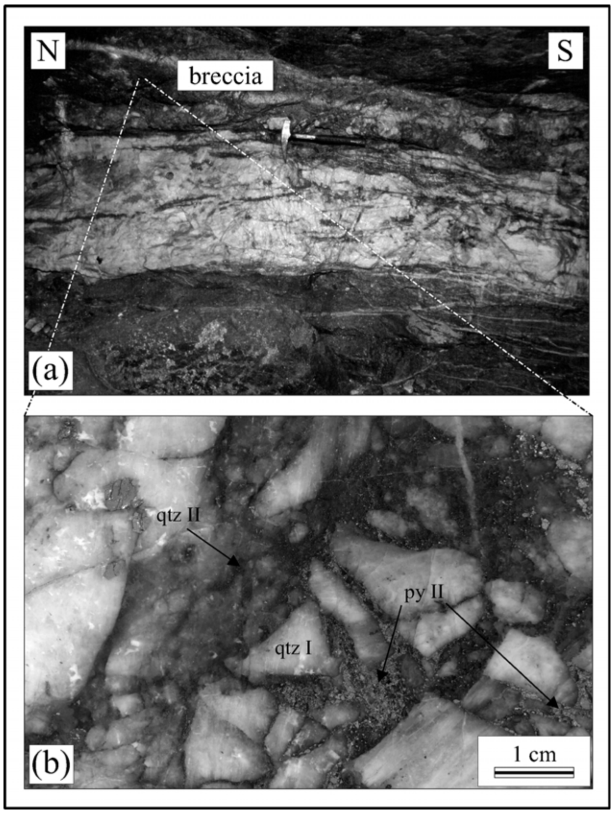

Fig. 12. (a) Looking east, down the dip of the Maude St Ledger Reef. The vein comprises an upper brecciated and a lower laminated portion and is accompanied by minor quartz veins. Both the tonalitic footwall and the vein are cut by millimeter- to centimeter-wide sheeted calcite veins; photograph kindly provided by Simon Dominy. (b) Breccia specimen from the Maude St Ledger Reef consisting of millimeter- to centimeter-wide clasts of primary vein quartz (qtz I). The fragments are contained within a matrix of gray quartz (qtz II) and paragenetically late pyrite (py II).

Repeated movement is also indicated by the reverse separation of a portion of the Maude St Ledger Reef. The displacement occurred most likely after ore deposition as the vein fragment contains the complete quartz–sulfide–calcite paragenesis. During this event, the upper surface of the Maude St Ledger acted as a shear horizon upon which the fragment was likely thrusted; a proposition made on the basis of folded sheeted calcite veins (Fig. 13). Constraints on the timing of this fault episode are poor but given the folding of calcite veins and the inferred reverse dip-slip, one may suggest that deformation took place in an environment and at a depth level similar to that of gold mineralization. Therefore, faulting may have occurred late during D_4 and linked to the same tectonic regime as gold mineralization. Late displacement of vein portions is also evident at Hadleigh Castle, where the imbrication of vein segments resulted in the local thickening of the 01 Lode. Moreover, up to 20-cm-wide, sulfide-bearing vein fragments contained in fine grained gouge indicate that the host faults of the 01 and 02 Lodes were likely active after gold mineralization.

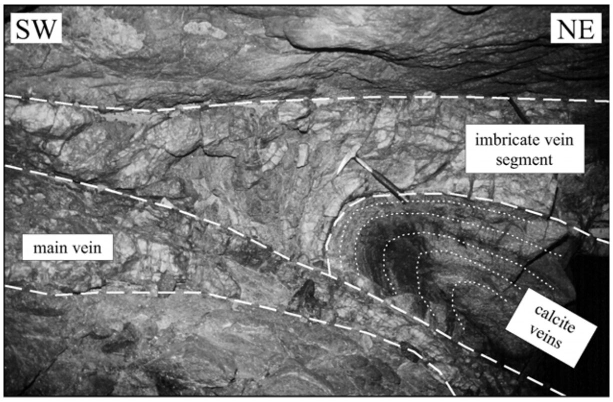

Fig. 13. Apparent reverse reactivation of the structure hosting the Maude St Ledger Reef indicated by an imbricate vein fragment. Folded sheeted calcite veins (dashed white lines) also indicate reverse movement. Thrusting possibly occurred late during D_4 and thus linked to the same tectonic regime as gold mineralization; photograph kindly provided by Simon Dominy.

7. The proposed structural model

Given the absence of vertical veins, abundance of flat-lying to shallow dipping veins and splay terminations, and preferential dilation and mineralization of shallower dipping vein segments, gold deposition in the CTGF likely occurred during regional shortening. Reverse separations of earlier structures cut by auriferous veins and the plunges of wear groove striations agree with the above proposition. Fault movements were apparently minor, that is on a centimeter to meter scale. Such an estimate is implied by the distances between observed reverse separations and is in agreement with Reid (1917), who reported average separations in the order of 0.9–1.2 m. Overall, the field data indicate a regime of NNE–SSW to ENE–WNW directed shortening during D_4 (Fig. 8).

8. Analysis of fault-slip data

Fault plane solutions and an extension of the right dihedra or P/T quadrant method (e.g. Ramsay and Lisle, 2000, and references therein), namely the AB dihedra solution of Lisle (1987), were used to analyze the fault-slip data. The AB dihedra solution was chosen as it provides a better resolution for small databases. Data were processed using FaultKinWin 1.1 (Allmendinger et al., 2001), following the kinematic approach of Marrett and Allmendinger (1990).

8.1. Fault plane solutions

As argued earlier, each of the measured wear groove striations apparently formed during quartz vein formation and gold deposition, or at least immediately after gold deposition during the same tectonic regime of regional shortening (D_4). Hence, fault plane solutions can be used to

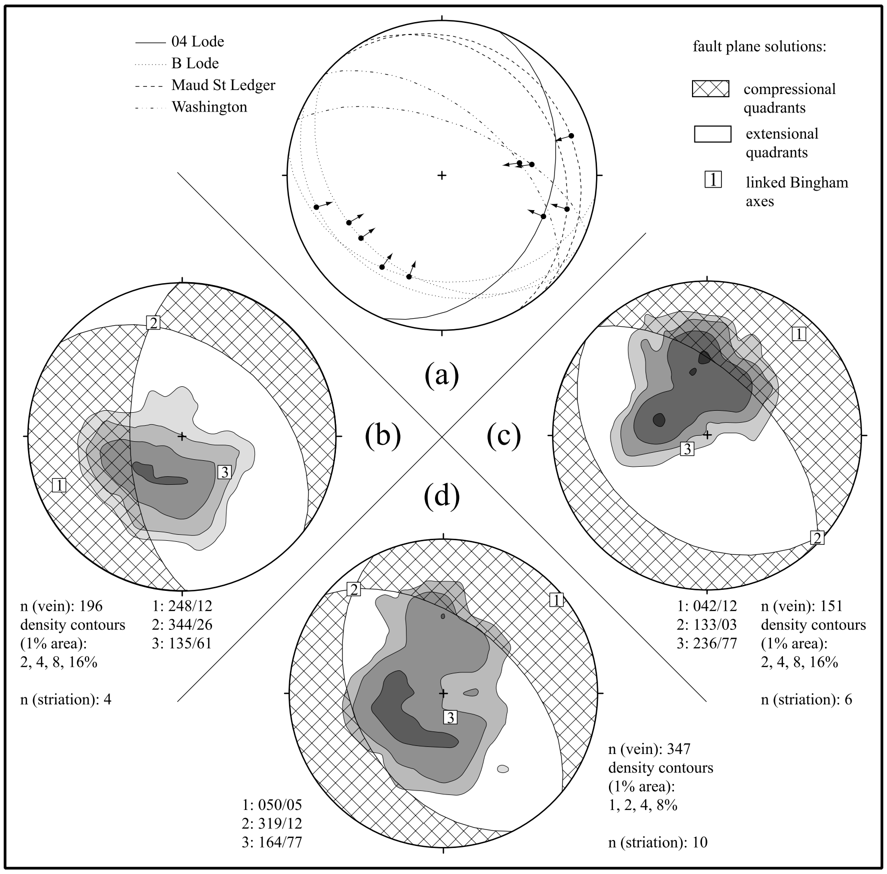

Fig. 14. (a) Lower hemisphere, equal area projection of measured wear groove striations and slip planes. Arrows indicate reverse senses of movement that, for each case, have been inferred from vein, splay termination and orebody geometries. (b) Fault plane solution for data from Charters Towers, also showing superimposed contours to poles of vein orientations. The latter plot mainly within the extensional quadrant. (c) A similar plot for data from Hadleigh Castle. (d) Fault plane solution for the combined data set.

identify the extensional and shortening quadrants. The principal strain axes are relatively consistent for both the individual and combined datasets, indicating NE–SW to ENE–WSW shortening during D_4. However, the orientations of the shortening axes may have varied up to $\pm 20°$ locally (Fig. 14). When superimposed on the fault plane solutions, contoured poles to vein orientations plot mainly within the extensional quadrants of the dihedra. Such a relationship is consistent with geological observations. Many of the studied veins appear to be extensional veins and extensional shear veins, characterized by shallow dips and comb quartz textures. Those veins plotting close to or within the shortening quadrants, for example the 01, 01$\frac{1}{2}$ and 02 Lodes (Hadleigh Castle), are often discontinuous. In addition, they commonly lack comb quartz but comprise breccia textures and deformed quartz and sulfides.

8.2. AB dihdra solutions

Individual solutions for Charters Towers and Hadleigh Castle imply a wide range of feasible fields containing the shortening axis, basically ranging from N–S to E–W. The matrix for the combined dataset on the other hand illustrates relatively narrow areas, consistent with a NE–SW to NNE–SSW directed distribution of shortening (Fig. 15).

9. Discussion

9.1. The structural model

Reid (1917) noted that "the comparative flatness of some of these fault fissures and the appearance of slickensided walls would certainly indicate that they were of the nature of overthrusts". However, based on a small number of normal separations of mafic dykes by auriferous veins, Reid (1917) proposed a link between gold mineralization and normal dip-slip. More recently, Peters (1987b) suggested that gold mineralization possibly occurred during reverse movement driven by NE–SW directed compression. The orientation of σ_1 given by Peters (1987b) was based on the assumption that N and E dipping veins would form what Peters (1987b) termed a 'shear couplet of reverse faulting'. However, the model was mainly based on the analysis of historic data and the failure criterion of intact rock, therefore neglecting the potential consequences of reactivation.

In contrast to Peters (1987a,b), whose research focused

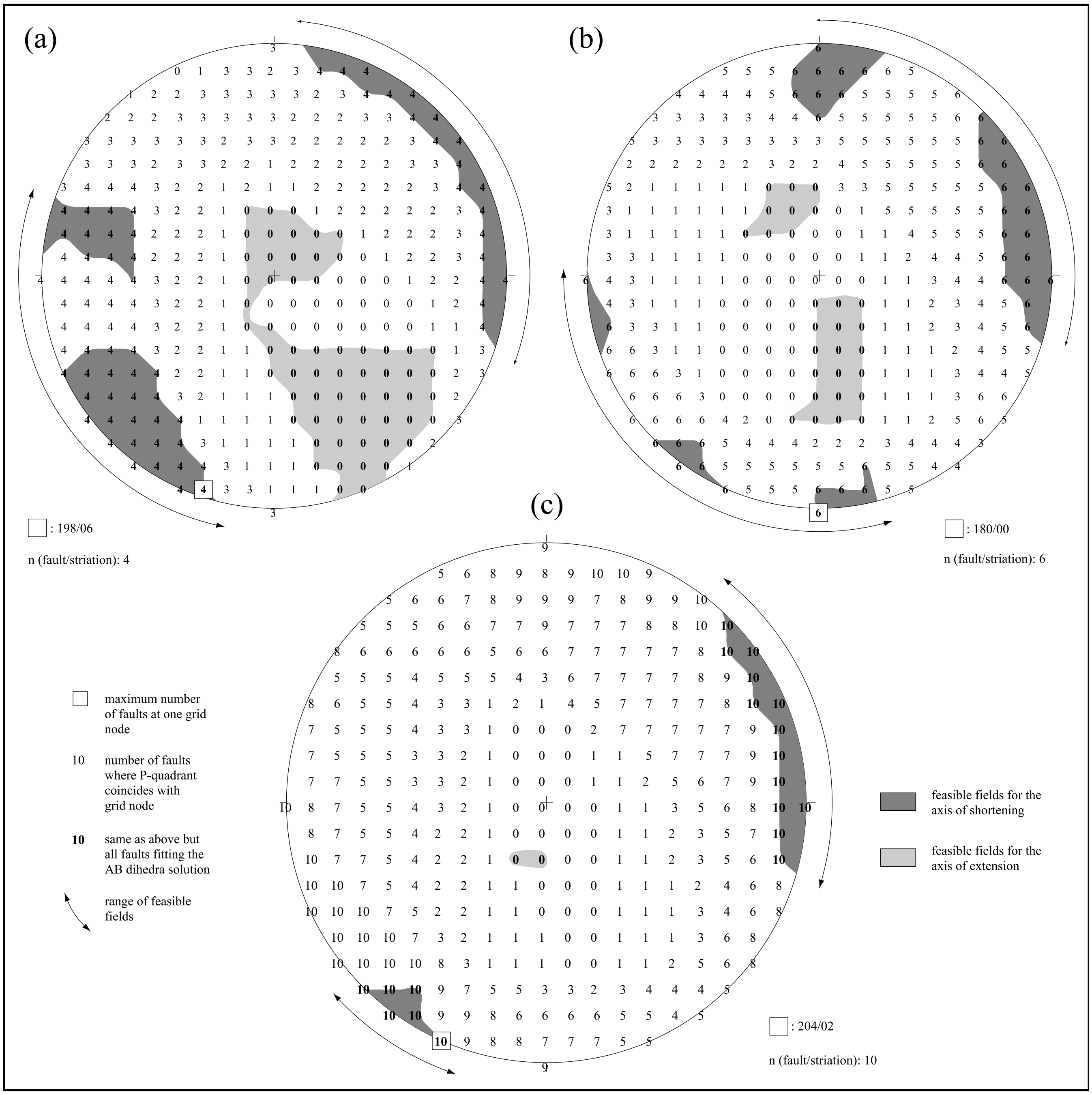

Fig. 15. AB P-dihedra solutions. (a) Data from Charters Towers illustrating a wide range of the feasible fields containing the shortening and extension axes. (b) Data from Hadleigh Castle show a similarly wide range. (c) The combined data set results in relatively narrow feasible fields consistent with a NE–SW to NNE–SSW range of the axis of shortening.

on the city of Charters Towers, the current study covered about 400 km^2 of the historic CTGF, including several accessible mines. The extracted structural data are remarkably consistent and together with the comparable alteration assemblages and textural, mineralogical, and paragenetic similarities implies synchronous formation of auriferous veins in the CTGF. However, the control of gold deposition by pre-existing structures accounts for some variability, such as opposing dip directions of E–W to ENE–WSW striking veins at Charters Towers and Hadleigh Castle. Ubiquitous flat-lying to shallow dipping veins and splay terminations, the lack of vertical veins, and the preferential dilation and mineralization of shallower dipping vein segments in the CTGF are consistent with the geometries of veins and fractures that formed during regional shortening (cf. fig. 14 in Cox et al., 2001; fig. 25 in Robert and Poulsen, 2001; fig. 15 in Sibson, 2001). An implication of the newly proposed oblique reverse movement during gold deposition is that left or right steps in host structures may have provided favorable sites for ore deposition in releasing or restraining bends or jogs, respectively. Moreover, ore-shoots may have preferentially formed where left or right steps in the host structures coincide with a marked shallowing of the vein structure.

Due to lacking kinematic indicators, reverse separations of earlier structures cut by auriferous veins could not be demonstrably linked to reverse slip. Secondly, the synchronicity of wear groove striations and gold mineralization could not be established beyond doubt. However, the data are consistent. Furthermore, they are in agreement with the proposed regional shortening regime and the single episode of vein formation and gold mineralization during D_4. As outlined earlier, the shallow dipping host structures of some auriferous veins were apparently reactivated during D_4. Hence, if the reverse separations and wear groove striations did not record fault movement during gold mineralization, they likely recorded fault-slip occurring after gold deposition but possibly driven by the same tectonic forces. There is no evidence for post-D_4 deformations causing any reactivation of the shallow to moderately dipping fractures hosting the bulk of the auriferous veins. Moreover, post-D_4 deformations produced steep dipping to vertical strike-slip, reverse and normal separations cutting the auriferous veins.

9.2. Reactivation of earlier structures and the role of fluid pressure

In the case of the RAB, the reactivation of pre-existing discontinuities is a recurring theme throughout its Early Palaeozoic history and, more importantly, intimately linked to Siluro-Devonian quartz vein formation and gold deposition. The nature of quartz–sulfide veins in the Sabie–Pilgrim's Rest Goldfield (Harley and Charlesworth, 1996) may help to develop an understanding, as the latter are in many respects similar to auriferous veins in the CTGF. Comparable features include open-space filling textures, in particular vugs lined with concentric comb quartz layers. Secondly, shallow dipping faults in both goldfields were repeatedly reactivated and, linked to this process, subject to episodic ore precipitation. Thirdly, auriferous veins in both goldfields were, after the main stage of vein development, locally deformed by continued reverse faulting. Based on their textures and geological history, Harley and Charlesworth (1996) concluded that the reactivation of fault-hosted veins in the Sabie–Pilgrim's Rest Goldfield was most likely assisted by overpressured fluids that were also regarded as crucial for maintaining dilatancy (cf. Sibson, 1996) and for faulting to occur under supposedly low strain.

When taking into consideration that (a) much of the gold mineralization is fully or partially hosted by pre-existing discontinuities, (b) shallow dipping to flat-lying mineralized hydraulic extension fractures are abundant, (c) the latter and ore-bearing low displacement faults are interconnected, (d) displacement values are apparently minor (centimeter to meter scale), and that (e) repeated movements occurred on host structures during ore-shoot formation, auriferous veins in the CTGF resemble so-called fault-fracture meshes (e.g. Sibson, 1996; Sibson and Scott, 1998). For such meshes to evolve, specific conditions are required that further constrain the environment of fault reactivation during Siluro-Devonian quartz vein formation and gold deposition in the CTGF. Sibson (1996) described these fault–fracture meshes as 'self-generated', meaning they possibly evolved by fault-valve action. The latter process is linked to (e.g. earthquake triggered) rupturing of an impermeable seal that until that time maintained an area of fluid pressures above hydrostatic. The penetration of the seal then permits fluids to migrate from the overpressured zone into the surrounding hydrostatic environment (Demming, 2002). Sibson et al. (1988) regarded the brittle carapaces of regions undergoing prograde regional metamorphism as such seals. When penetrated, overpressured fluids can migrate into the stressed crust potentially comprising an array of pre-existing discontinuities. Over time and by progressive fluid induced rock failure these discontinuities may become gradually interlinked, thus promoting the permeability of the rock mass and the formation of continuous faults (Sibson, 1996). Dropping fluid pressures may then trigger mineral deposition, hence sealing the cracks and potentially initiating a repetition of the cycle (Sibson et al., 1988). The prerequisites for fault–fracture mesh evolution in compressional settings are fluid pressures approaching or exceeding lithostatic levels or extreme stress heterogeneities, for instance caused by the variability of local and far field stress fields (Sibson, 1996). Given the (a) proposed depth of quartz vein formation and gold deposition in the CTGF, (b) inferred compressional regime and minor reverse movement on host faults, (c) wealth of open-space filling textures, (d) evidence for fluid-assisted brecciation due to hydraulic or critical fracturing (cf. Jebrak, 1997), (e) abundance of shallow dipping to flat-lying veins, and (f) lacking evidence for variable local and far field stress fields, it seems likely that the pressures of the ore-bearing fluids were near-lithostatic to supralithostatic.

According to Sibson (1996, 2000) and Sibson and Scott (1998), in compressional regimes, where the vertical stress (σ_v) equals the least principal stress (σ_3), formation of flat-lying fractures requires supralithostatic pressures at all depths. Given the abundance of such flat-lying vein arrays (e.g. Robinson Crusoe Pit) and splay terminations (e.g. Hadleigh Castle Mine) in the CTGF, it seems more than likely that the ore-bearing fluids were overpressured. When applying the models presented by Sibson (1985) and Sibson and Scott (1998) to the CTGF, it becomes obvious that many of the pre-existing discontinuities in the CTGF would have been misoriented in the compressive stress field present at the time of gold mineralization. For instance, the reactivation angle (θ_r) of steeply dipping mafic dyke swarms at Charters Towers would have been more than twice the optimal value (i.e. $\theta_r > 50$–$60°$). However, Sibson (1985) and Sibson and Scott (1998) argued that such misoriented structures are fundamental for hydraulic extension fracturing and fault–fracture mesh formation to occur.

9.3. The graphical methods

The shape diagram (cf. Blenkinsop, 2004, this volume) proved to be a simple and practical tool for systematic delineation of ore-shoot populations. Furthermore, by building a database and constantly evaluating the preliminary groupings, the shape diagram may also be used in a predictive fashion; that is to estimate the dimensions of open or poorly defined ore-shoots. Here, four distinct populations were revealed. Group I orebodies have mainly prolate shapes. In particular, they represent tubular or potentially tubular zones of high fracture density dominated by a single long axis (*U*). In the case of the stockwork veins accompanying the Golden Alexandra, Stockholm and Robinson Crusoe Reefs, *U* corresponds to the strike axes of these stockworks. The Hadleigh Castle Vein System, however, is governed by its dip axis. Given the inferred orientation of the shortening axis (i.e. NE–SW ± 20°), the *U* axes of the stockworks were either at high angles, subparallel or nearly perpendicular to the shortening axis. Conversely, the *U* axis of the Hadleigh Castle Vein System was slightly oblique to nearly perpendicular to the shortening axis.

Ore-shoots assigned to Groups II–IV are oblate and have decreasing *j* values governed by increasing *V*/*W* ratios. Their *U* axes coincide with either their strike or dip extent. Similar to Group I, Groups II–IV ore-shoots do not show any particular pattern of alignment with respect to the orientation of the shortening axis. Their *U* axes were variably oriented subparallel to roughly perpendicular to the shortening axis. Therefore, with the available data, no obvious link could be established between the orientation of the shortening and *U* axes and the ore-shoot size. However, since many orebodies appear to be controlled by pre-existing discontinuities a straightforward relationship would have been surprising.

The differing shapes of the orebodies of Group I and Groups II–IV may indicate that, locally, fluid flow was controlled by a growing fracture network with an overall tubular shape. When reaching the percolation threshold (e.g. Cox et al., 2001), fluids may have been channeled from the tubular fracture network into single tabular fractures. Such a scenario would also account for the abundance of poorly mineralized veins and stockwork veins since ore precipitation would have been restricted to a small subset of the whole fracture population. However, the systems may have evolved from tabular to tubular and further work will be necessary to evaluate the above proposition.

Kinematic analysis of fault-slip data can assist with developing a more objective strain model than one based on the interpretation of field data alone. Furthermore, a number of authors (e.g. Gapais et al., 2000, and references therein) argued that a kinematic approach revealing the principal axis of strain is generally more reliable than a dynamical one. Similar to the shape diagram of Blenkinsop (2004, this volume), fault plane and AB dihedra solutions are simple and practical tools. If possible, field data collection should include the orientation of the fault plane, slip direction, sense of slip, average displacement, and fault area. These measurements should be obtained from a planar segment of the fault, approximating the mean fault orientation (Marrett and Allmendinger, 1990). Therefore, data from the CTGF are non-ideal as the wear groove striations yielded no indication as to whether dip-slip was normal or reverse. However, for each occurrence reverse dip-slip has been inferred on the basis of vein and ore-shoot geometries. Likewise, the link between wear groove striations and gold deposition could not be established beyond doubt. Nevertheless, the data are consistent and there is reasonable evidence for wear groove striations having formed during D_4, and thus during the same tectonic regime and strain field as gold deposition.

10. Conclusions

Based on the structural and kinematic analysis of auriferous veins in the CTGF the following conclusions can be drawn:

(a) Flat-lying to shallow dipping splay terminations, and preferential dilation and mineralization of shallower dipping vein segments are consistent with models for ore deposition during regional shortening.
(b) Wear groove striations imply pure to oblique dip-slip movement on host faults. The oblique component possibly resolved in reverse dextral shear on E dipping and reverse sinistral slip on N dipping host faults.
(c) Reactivated planes of weakness host a number of auriferous veins at Charters Towers and Hadleigh Castle. The importance of earlier discontinuities is also implied by the widespread coincidence of vein orientations and structures that formed prior to gold mineralization. E–W and NNW–SSE striking planes of weakness were possibly oriented most favorably for reactivation during D_4, thus providing important loci for quartz vein formation and ascent of ore-bearing fluids.
(d) The shape diagram proved to be a useful tool for systematic ore-shoot comparison, also suggesting that the richest ore-shoots have the lowest *j* values.
(e) Fault plane and AB dihedra solutions further constrained the geological model. Outcomes are consistent with a NE–SW (± 20°) orientation of the shortening axis during the time of gold mineralization.
(f) In some cases, the scarcity of kinematic data and issues of fault reactivation may be overcome by extracting

geometrical information from the orebodies and developing a geological model that can be used for or tested by graphical analysis.

Acknowledgements

The author acknowledges International Postgraduate Research and School of Earth Sciences Scholarships and financial support from supervisors Nick Oliver and Andrew Allibone. The latter and Simon Dominy are thanked for kindly providing underground photographs. Suggestions from and a review by Tom Blenkinsop helped to greatly improve the quality of the analyses and the manuscript. Constructive reviews by Michel Jebrak and Gerard Tripp are greatly appreciated, also improving the manuscript significantly. Jim Morrison, Nigel Storey and Kris Butera (Charters Towers Gold Mines Ltd), Ian Hodkinson, Harry Mustard and Stuart Hampton (SMC Gold Ltd), and Tony Alston (Glengarry Resources Ltd) are thanked for their support and granted access to company data and leases.

References

Allibone, A., Teasdale, J., Cameron, G., Etheridge, M., Uttley, P., Soboh, A., Appiah-Kubi, J., Adanu, A., Arthur, R., Mamphey, J., Odoom, B., Zuta, J., Tsikata, A., Pataye, F., Famiyeh, S., 2002. Timing and structural controls on gold mineralization at the Bogoso Mine, Ghana, West Africa. Economic Geology 97, 949–969.

Allmendinger, R.W., Marrett, R.A., Cladouhos, T., 2001. FaultKinWin Version 1.1; a Program for Analyzing Fault Slip Data for Windows Computers. Copyright © Allmendinger, R.W., 1989–2001.

Baker, T., 2003. Lindgren's legacy: magmas, fluids and ore deposits. In: Baker, T., Cleverly, J.S., Fu, B. (Eds.), Magmas, Fluids and Porphyry-Epithermal Deposits. Contributions of the Economic Geology Research Unit, James Cook University, Townsville 61, pp. 1–12.

Benn, K., Odonne, F., de Saint Blanquat, M., 1998. Pluton emplacement during transpression in brittle crust: new views from analogue experiments. Geology 26, 1079–1082.

Berry, R.F., Huston, D.L., Stolz, A.J., Hill, A.P., Beams, S.D., Kuronen, U., Taube, A., 1992. Stratigraphy, structure, and volcanic-hosted mineralization of the Mount Windsor Subprovince, north Queensland, Australia. Economic Geology 87, 739–763.

Blatchford, A., 1953. Charters Towers Goldfield. In: Proceedings of the Empire Mining and Metallurgical Congress 1, pp. 796–806.

Blenkinsop, T.G., 2000. Deformation Microstructures and Mechanics in Minerals and Rocks. Kluwer Academic Publishers, Dordrecht.

Blenkinsop, T.G., 2004. Orebody geometry in lode gold deposits from Zimbabwe: implications for fluid flow, deformation and mineralization. Journal of Structural Geology, 2004.001:10.1016/j.jsg2003.11.010.

Carr, G.R., Dean, J.A., Morrison, G.W., 1988. Lead isotopes as an exploration technique and an aid in genetic modeling for gold deposits in northeast Queensland. In: Goode, A.D.T., Bosma, L.I. (Eds.), Bicentennial Gold '88, Geological Society of Australia Abstracts, Melbourne, 22, pp. 265–271.

Cassidy, K.F., Bennet, J.M., 1993. Gold mineralization at the Lady Bountiful mine, Western Australia: an example of a granitoid-hosted Archaean lode gold deposit. Mineralium Deposita 28, 388–408.

Cox, S.F., Wall, V.J., Etheridge, M.A., Potter, T.F., 1991. Deformational and metamorphic processes in the formation of mesothermal vein-hosted gold deposits—examples from the Lachlan Fold Belt in central Victoria, Australia. Ore Geology Reviews 6, 391–423.

Cox, S.F., Knackstedt, M.A., Braun, J., 2001. Principles of structural control on permeability and fluid flow in hydrothermal systems. In: Richards, J.P., Tosdal, R.M. (Eds.), Structural Controls on Ore Genesis. Reviews in Economic Geology, Society of Economic Geologists, Littleton, 14, pp. 1–24.

Cruden, A.R., 1998. On the emplacement of tabular granites. Journal of the Geological Society of London 155, 853–862.

Demming, D., 2002. Chapter 7: Driving Forces for Fluid Flow. http://www.edge.ou.edu/ ydrogeology/page13.html.

Dowling, K., Morrison, G.W., 1989. Application of quartz textures to the classification of gold deposits using North Queensland examples. In: Keays, R.R., Ramsay, W.R.H., Groves, D.I. (Eds.), The Geology of Gold Deposits: the Perspective in 1988. Economic Geology Monograph, Society of Economic Geologists, Littleton, 6, pp. 342–355.

Forde, A., Bell, T.H., 1994. Late structural control of mesothermal vein-hosted gold deposits in Central Victoria, Australia: mineralization mechanisms and exploration potential. Ore Geology Reviews 9, 33–59.

Gapais, D., Cobbold, P.R., Bourgeois, O., Rouby, D., de Urreiztieta, M., 2000. Tectonic significance of fault-slip data. Journal of Structural Geology 22, 881–888.

Goldfarb, R.J., Phillips, G.N., Nokleberg, W.J., 1998. Tectonic setting of synorogenic gold deposits of the Pacific Rim. Ore Geology Reviews 13, 185–218.

Goldfarb, R.J., Groves, D.I., Gardoll, S., 2001. Orogenic gold and geologic time: a global synthesis. Ore Geology Reviews 18, 1–75.

Groves, D.I., Goldfarb, R.J., Gebre-Mariam, M., Hagemann, S.G., Robert, F., 1998. Orogenic gold deposits: a proposed classification in the context of their crustal distribution and relationship to other gold deposit types. Ore Geology Reviews 13, 7–27.

Hammond, R.L., 1986. Large scale structural relationships in the Palaeozoic of northeastern Queensland: melange and mylonite development, and the regional distribution of strain. Ph.D. thesis, James Cook University, Townsville, Australia.

Harley, M., Charlesworth, E.G., 1996. The role of fluid pressure in the formation of bedding-parallel, thrust-hosted gold deposits, Sabie–Pilgrim's Rest Goldfield, eastern Transvaal. Precambrian Research 79, 125–140.

Hartley, J.S., 1996. Mineral occurrences—Ravenswood 1:100,000 sheet area. Queensland Geological Record, Department of Minerals and Energy, Brisbane, 1996/2.

Hartley, J.S., Dash, P.H., 1993. Mineral occurrences–Charters Towers 1:100,000 sheet area. Queensland Geological Record, Department of Minerals and Energy, Brisbane, 1993/6.

Heidecker, E., 1974. A review of major Palaeozoic tectonometallogenic events, northern part of the Tasman Orogenic Zone. In: Denmead, A.K., Tweedale, G.W., Wilson, A.F. (Eds.), The Tasman Geosyncline–A Symposium, Geological Society of Australia, Brisbane, pp. 99–128.

Henderson, R.A., 1980. Structural outline and summary of geological history for northeastern Australia. In: Henderson, R.A., Stephenson, P.J. (Eds.), The Geology and Geophysics of Northeastern Australia, Geological Society of Australia, Brisbane, pp. 1–26.

Henderson, R.A., Davis, B.K., Fanning, C.M., 1998. Stratigraphy, age relationships and tectonic setting of rift-phase infill in the Drummond Basin, central Queensland. Australian Journal of Earth Sciences 45, 579–595.

Hodgson, C.J., 1989. The structure of shear-related, vein-type gold deposits: a review. Ore Geology Reviews 4, 231–273.

Hodkinson, I.P., 1998. Geology of the Hadleigh Castle Mine, Charters Towers. In: Beams, S.D., (Ed.), Economic Geology of northeast Queensland: the 1998 Perspective, Geological Society of Australia, Melbourne, pp. 230–241.

Hutton, L.J., Rienks, I.P., 1997. Geology of the Ravenswood Batholith. Queensland Geology, Department of Mines and Energy, Brisbane, 8.

Hutton, L.J., Draper, J.J., Rienks, I.P., Withnall, I.W., Knutson, J., 1997. Charters Towers region. In: Bain, J.H.C., Draper, J.J. (Eds.), North

Queensland Geology. Australian Geological Survey Organization Bulletin 240, pp. 165–224.

Jack, R.L., Rands, W.H., Maitland, A.G., 1898. Geological map of the Charters Towers Goldfield. Geological Survey of Queensland Publication, Brisbane, 142.

Jebrak, M., 1997. Hydrothermal breccias in vein-type ore deposits: a review of mechanisms, morphology and size distribution. Ore Geology Reviews 12, 111–134.

Levingston, K.R., 1972. Ore deposits and mines of the Charters Towers 1:250,000 sheet area, north Queensland. Geological Survey of Queensland Report, Brisbane, 57.

Lindgren, W., 1933. Mineral Deposits, 4th ed, McGraw-Hill, New York.

Lisle, R.J., 1987. Principal stress orientations from faults: an additional constraint. Annales Tectonicae 1, 155–158.

Marrett, R., Allmendinger, R.W., 1990. Kinematic analysis of fault-slip data. Journal of Structural Geology 12, 973–986.

McKeagney, C.J., Foster, R.P., Boulter, C.A., 1997. Structural controls of gold mineralization at the Indarama Mine, Zimbabwe: a key to the evolution of a world-class gold camp. In: Papunen, H., (Ed.), Mineral Deposits: Research and Exploration, Where Do They Meet?, Balkema, Rotterdam, pp. 241–244.

Miller, J.McL., Wilson, C.J., 2002. The Magdala Lode System, Stawell, southeastern Australia: structural style and relationship to gold mineralization across the Lachlan Fold Belt. Economic Geology 97, 325–349.

Murray, C.G., Kirkegaard, A.G., 1978. The Thomson Orogen of the Tasman Orogenic Zone. Tectonophysics 48, 299–325.

Perkins, C., Kennedy, A.K., 1998. Permo-Carboniferous gold epoch of northeast Queensland. Australian Journal of Earth Sciences 45, 185–200.

Peters, S.G., 1987a. Geology, fluid characteristics, lode controls and ore-shoot growth in mesothermal gold-quartz veins, north-eastern Queensland. Ph.D. thesis, James Cook University, Townsville, Australia.

Peters, S.G., 1987b. Geology and lode controls of the Charters Towers Goldfield, northeastern Queensland. Contributions of the Economic Geology Research Unit, James Cook University, Townsville, 19.

Peters, S.G., Golding, S.D., 1989. Geologic, fluid inclusion and stable isotope studies of granitoid-hosted gold-bearing quartz veins, Charters Towers, northeastern Australia. In: Keays, R.R., Ramsay, W.R.H., Groves, D.I. (Eds.), The Geology of Gold Deposits: the Perspective in 1988. Economic Geology Monograph, Society of Economic Geologists, Littleton, 6, pp. 260–273.

Ramsay, J.G., Lisle, R.J., 2000. The Techniques of Modern Structural Geology, Volume 3: Applications of Continuum Mechanics in Structural Geology. Academic Press, London.

Reid, J.H., 1917. The Charters Towers Goldfield. Geological Survey of Queensland Publication, Brisbane, 256.

Richards, D.N.G., 1980. Palaeozoic granitoids of northeastern Australia. In: Henderson, R.A., Stephenson, P.J. (Eds.), The Geology and Geophysics of Northeastern Australia, Geological Society of Australia, Brisbane, pp. 229–246.

Rienks, I.P., Beams, S.D., Rapkins, R.J., 1996. Ravenswood Special, Queensland. Queensland Department of Mines and Energy Map 8257 and part of 8357, 8256 and 8356, scale 1:100,000.

Robert, F., Poulsen, K.H., 2001. Vein formation and deformation in Greenstone Gold Deposits. In Richards, J.P., Tosdal, R.M. (Eds.), Structural Controls on Ore Genesis. Reviews in Economic Geology, Society of Economic Geologists, Littleton, 14, pp. 111–155.

Scheibner, E., Veevers, J.J., 2000. Tasman Fold Belt System. In: Veevers, J.J., (Ed.), Billion-year Earth History of Australia and Neighbors in Gondwanaland, Gemoc Press, Sydney, pp. 154–233.

Sibson, R.H., 1985. A note on fault reactivation. Journal of Structural Geology 7, 751–754.

Sibson, R.H., 1996. Structural permeability of fluid-driven fault-fracture meshes. Journal of Structural Geology 18, 1031–1042.

Sibson, R.H., 2000. A brittle failure mode plot defining conditions for high-flux flow. Economic Geology 95, 41–48.

Sibson, R.H., 2001. Seismogenic framework for hydrothermal transport and ore deposition. In: Richards, J.P., Tosdal, R.M. (Eds.), Structural Controls on Ore Genesis. Reviews in Economic Geology, Society of Economic Geologists, Littleton, 14, pp. 25–50.

Sibson, R.H., Scott, J., 1998. Stress/fault controls on the containment and release of overpressured fluids: examples from gold–quartz vein systems in Juneau, Alaska; Victoria, Australia and Otago, New Zealand. Ore Geology Reviews 13, 293–306.

Sibson, R.H., Robert, F., Poulsen, K.H., 1988. High-angle reverse faults, fluid pressure cycling, and mesothermal gold-quartz deposits. Geology 16, 551–555.

Solomon, M., Groves, D.I., 2000. The geology and origins of Australia's mineral deposits. Centre for Ore Deposit Research (University of Tasmania) and Centre for Global Metallogeny (University of Western Australia) Publication 32, 661–666.

Tenison-Woods, K.L., Rienks, I.P., 1992. New insights into the structure and subdivision of the Ravenswood Batholith—a geophysical perspective. Exploration Geophysics 23, 353–360.

Vearncombe, J.R., 1998. Shear zones, fault networks and Archaean gold. Geology 26, 855–858.

Wellman, P., 1995. Tasman Orogenic System: a model for its subdivision and growth history based on gravity and magnetic anomalies. Economic Geology 90, 1430–1442.

Withnall, I.W., Lang, S.C., 1993. Geology of the Broken River Province, north Queensland. Queensland Geology Department of Mines and Energy, Brisbane, 4.